Science Signaling
AAAS

` Dysregulated RasGRP1 Responds to Cytokine Receptor Input in T Cell Leukemogenesis

Catherine Hartzell, Olga Ksionda, Ed Lemmens, Kristen Coakley, Ming Yang, Monique Dail, Richard C. Harvey, Christopher Govern, Jeroen Bakker, Tineke L. Lenstra, Kristin Ammon, Anne Boeter, Stuart S. Winter, Mignon Loh, Kevin Shannon, Arup K. Chakraborty, Matthias Wabl and Jeroen P. Roose (26 March 2013)

Science Signaling **6** (268), ra21. [DOI: 10.1126/scisignal.2003848]

Science Signaling (ISSN 1937-9145) is published weekly, except the last week in December, by the American Association for the Advancement of Science, 1200 New York Avenue, NW, Washington, DC 20005.

CANCER

Dysregulated RasGRP1 Responds to Cytokine Receptor Input in T Cell Leukemogenesis

Catherine Hartzell,[1]* Olga Ksionda,[1]* Ed Lemmens,[1]* Kristen Coakley,[1] Ming Yang,[2] Monique Dail,[3] Richard C. Harvey,[4] Christopher Govern,[2] Jeroen Bakker,[1] Tineke L. Lenstra,[1] Kristin Ammon,[3] Anne Boeter,[1] Stuart S. Winter,[5] Mignon Loh,[3] Kevin Shannon,[3] Arup K. Chakraborty,[2,6,7,8,9] Matthias Wabl,[10] Jeroen P. Roose[1]†

Enhanced signaling by the small guanosine triphosphatase Ras is common in T cell acute lymphoblastic leukemia/lymphoma (T-ALL), but the underlying mechanisms are unclear. We identified the guanine nucleotide exchange factor RasGRP1 (Rasgrp1 in mice) as a Ras activator that contributes to leukemogenesis. We found increased *RasGRP1* expression in many pediatric T-ALL patients, which is not observed in rare early T cell precursor T-ALL patients with *KRAS* and *NRAS* mutations, such as *K-Ras*^{G12D}. Leukemia screens in wild-type mice, but not in mice expressing the mutant *K-Ras*^{G12D} that encodes a constitutively active Ras, yielded frequent retroviral insertions that led to increased *Rasgrp1* expression. Rasgrp1 and oncogenic *K-Ras*^{G12D} promoted T-ALL through distinct mechanisms. In *K-Ras*^{G12D} T-ALLs, enhanced Ras activation had to be uncoupled from cell cycle arrest to promote cell proliferation. In mouse T-ALL cells with increased *Rasgrp1* expression, we found that Rasgrp1 contributed to a previously uncharacterized cytokine receptor–activated Ras pathway that stimulated the proliferation of T-ALL cells in vivo, which was accompanied by dynamic patterns of activation of effector kinases downstream of Ras in individual T-ALLs. Reduction of Rasgrp1 abundance reduced cytokine-stimulated Ras signaling and decreased the proliferation of T-ALL in vivo. The position of RasGRP1 downstream of cytokine receptors as well as the different clinical outcomes that we observed as a function of RasGRP1 abundance make RasGRP1 an attractive future stratification marker for T-ALL.

INTRODUCTION

T cell acute lymphoblastic leukemia/lymphoma (T-ALL) is an aggressive cancer of children and adults (*1*). Although dose-intensive therapies have markedly improved the outcomes in children and adolescents with T-ALL, the cure rates for adults with T-ALL remain less than 50%, and the prognosis is poor for patients that relapse at any age (*1*, *2*). Modern genotoxic treatment regimens also carry a substantial risk of treatment-related toxicity or adverse late effects (*3*). Thus, the development of more effective and less toxic therapeutic agents that are based on the underlying molecular pathogenesis is a high priority. However, T-ALL is a heterogeneous disease with diverse and complex cytogenetic abnormalities (*4*–*6*) and variable developmental stages (*7*), which likely will complicate the identification of universal target molecules. Gene expression microarray studies also point to distinct developmental stages in T-ALL (*8*). In contrast to the successful stratification of diffuse large B cell lymphomas (*9*), attempts to stratify T-ALL on the basis of developmental markers have not yet been fruitful (*4*, *10*–*12*).

Enhanced signaling by the small guanosine triphosphatase (GTPase) Ras is implicated in the pathogenesis of ~50% of T-ALL cases (*13*), but the molecular mechanisms causing aberrant Ras signaling in T-ALL are not well understood. Ras is normally activated by guanosine triphosphate (GTP) loading by Ras guanine nucleotide exchange factors (RasGEFs), which include Son of Sevenless (SOS), Ras guanine nucleotide–releasing protein (RasGRP), and Ras guanine nucleotide–releasing factor (RasGRF) (*14*). The intrinsic, deactivating GTPase activity of Ras is strongly enhanced by critical inhibitors of Ras, the Ras GTPase-activating proteins (RasGAPs) (*15*). Somatic mutations in the gene encoding Ras that result in an accumulation of the GTP-bound form of the Ras protein are among the most frequent oncogenic lesions in metastasizing disease (*16*). Biochemically, these mutations, such as *K-Ras*^{G12D}, lead to a severely impaired GTPase activity of Ras (*17*) that is no longer enhanced by RasGAPs. For unknown reasons, somatic *NRAS* and *KRAS* mutations are relatively rare in T-ALL (*18*–*20*), accounting for only ~10% of T-ALL cases, which leaves a large proportion of the T-ALL cases with enhanced Ras activation (*13*) that are unexplained.

Three studies have uncovered important insights regarding the role of Ras and cytokine signaling in T-ALL. Whole-genome sequencing revealed that *NRAS* and *KRAS* mutations, as well as activating mutations in *Janus activating kinase 1* (*JAK1*) and *JAK3* or activating mutations in *IL7R* [which encodes the interleukin-7 receptor (IL-7R)], occur with much higher frequency in a specific subtype of T-ALL, early T cell precursor (ETP) T-ALL, which is typically associated with a poor clinical outcome (*21*). Biochemically, these T-ALL IL-7R mutations result in constitutive activation of the kinase JAK1 downstream of the receptor independently of IL-7 binding, which leads to cellular transformation and tumor formation (*22*). The connection between IL-7 and T-ALL was further substantiated

[1]Department of Anatomy, University of California, San Francisco, San Francisco, CA 94143, USA. [2]Department of Chemical Engineering, Massachusetts Institute of Technology, 77 Massachusetts Avenue, Cambridge, MA 02139, USA. [3]Department of Pediatrics, University of California, San Francisco, San Francisco, CA 94143, USA. [4]Department of Pathology, University of New Mexico School of Medicine, MSC 10 5590, Albuquerque, NM 87131, USA. [5]Department of Pediatrics, University of New Mexico School of Medicine, MSC 10 5590, Albuquerque, NM 87131, USA. [6]Department of Chemistry, Massachusetts Institute of Technology, Cambridge, MA 02139, USA. [7]Department of Biological Engineering, Massachusetts Institute of Technology, Cambridge, MA 02139, USA. [8]Department of Physics, Massachusetts Institute of Technology, Cambridge, MA 02139, USA. [9]Institute for Medical Engineering and Science, Massachusetts Institute of Technology, Cambridge, MA 02139, USA. [10]Department of Immunology, University of California, San Francisco, San Francisco, CA 94143, USA.
*These authors contributed equally to this work.
†Corresponding author. E-mail: jeroen.roose@ucsf.edu

in a third study that showed that the proliferation of xenografted patient leukemia cells in the bone marrow and leukemia-associated morbidity are diminished in a mouse model that is deficient in IL-7 (*23*).

In contrast to ETP T-ALL (*21*), somatic *RAS* mutations are relatively rare in most T-ALL (*18*–*20*); however, Ras signaling is aberrantly high in 50% of cases (*13*). With analyses of pediatric T-ALL patient samples, investigation of common integration sites (CIS) in mouse leukemia virus screens, and biochemical assays aided by in silico methods, we found that Rasgrp1 is a frequently affected RasGEF in T-ALL. We found that increased Rasgrp1 protein abundance contributed to Ras activation in T-ALL in a manner that was biochemically distinct from that induced by oncogenic *K-Ras*^{G12D} mutations. Increased Rasgrp1 abundance alone resulted in only weak, basal Ras signaling that did not trigger cell cycle arrest. Instead, we found that increased Rasgrp1 abundance cooperated with cytokine receptor signaling to activate Ras and stimulate leukemogenesis. Last, we observed a high degree of heterogeneity in the activation of kinase pathways downstream of Ras, as well as evidence for plasticity in prosurvival signaling pathways in response to perturbations in Rasgrp1. We discuss how our data contrasting enhanced Rasgrp1 abundance with oncogenic *K-Ras*^{G12D} mutations provide new hypotheses and potential targets that can be exploited in the future to better understand how to intervene with different types of T-ALL Ras signaling with molecularly targeted therapeutic agents.

RESULTS

Computational analysis predicts that increased RasGRP catalytic rate results in enhanced Ras activation, whereas T-ALL patients display an extensive range in RasGRP1 mRNA abundance

Through computational analyses and cellular assays, we previously demonstrated that the RasGEF Rasgrp1 is necessary and sufficient to trigger Ras activation in lymphocytes, in contrast to Sos1, a Ras activator that functions best when Rasgrp1 is also present (*24*). To better understand how enhanced Ras signaling occurs in 50% of T-ALL cases, we used computational methods to simulate the activity of Rasgrp1. Given the identification of *NRAS* and *KRAS* mutations in ETP T-ALL (*21*), which occur with only low frequency in other T-ALLs (*18*–*20*), we explored what other biochemical events could, in principle, explain the enhanced Ras signaling in ~50% of T-ALL cases (*13*). We used our established computational models (fig. S1A) that stochastically simulate the Ras activation-deactivation cycle through Rasgrp, SOS, and RasGAP (*24*). To mimic *NRAS* or *KRAS* mutations that impair the GTPase activity of Ras (*17*), we decreased either the catalytic rate or the concentration of RasGAP in our model. As expected from the established inhibitory function of RasGAPs in the Ras activation-deactivation cycle (*15*), both impairments in RasGAP (catalytic activity and concentration) were predicted to lead to increases in the steady-state abundance of RasGTP at low, basal amounts of SOS (Fig. 1, A and B). These predictions remained the same when the constant amount of SOS activity was increased (fig. S1, B and C).

Next, we performed several perturbations of Rasgrp and SOS, and we noted that increases in the catalytic rate of Rasgrp also predicted substantial correlative increases in RasGTP abundance (Fig. 1A). In contrast, when we merely increased the number of Rasgrp molecules in the simulation, it did not increase the abundance of RasGTP accordingly, indicating that there was a parameter, in addition to the Rasgrp concentration, that was rate-limiting (Fig. 1B). As before (*24*), we used our computational models to formulate new hypotheses in this study, focusing on predictions of major characteristics. However, we did not concentrate on fitting the models to the biological data in terms of specific amplitude and timing of responses or specific concentrations of signaling molecules.

Increased *RasGRP1* mRNA abundance has been reported in microarray studies of primary human T-ALLs and cell lines (*19*, *25*, *26*). In contrast, *RasGRP1* expression is decreased in the ETP T-ALL subtype (*21*). We found that established human T-ALL lines exhibited a range of RasGRP1 protein abundance, showing up to a 10-fold increase compared to that in normal human T lymphocytes (Fig. 1C). These T-ALL lines represent a range of developmental stages on the basis of their cell-surface markers (*27*). When we examined primary patient samples, we confirmed the published microarray studies with real-time reverse transcription polymerase chain reaction (RT-PCR) analysis of 11 pediatric T-ALL patients. Six patients had increased *RasGRP1* mRNA abundance, whereas five patients had *RasGRP1* mRNA abundance that was similar to those of normal bone marrow donors (Fig. 1D). A similar small-scale survey also identified high *RasGRP1* expression in three of six T-ALL patients (*28*).

We subsequently investigated the expression patterns of all eight RasGEFs through the analysis of microarray data from 107 pediatric patients that were enrolled in the Children's Oncology Group (COG) studies 9900/9404 and AALL03B1/AALL0434. We observed a 128-fold range in *RasGRP1* expression (from 2^4 to 2^{11} in normalized array intensities, Fig. 1E). This extensive expression range was unique to *RasGRP1* and was not seen for the genes encoding the other seven RasGEFs (Fig. 1F). Graphing the extent of *RasGRP1* expression as a function of clinical outcome revealed an inverse correlation. With an arbitrary cutoff, 7 of 14 (50%) of patients that had low *RasGRP1* expression failed to achieve a first remission (induction failure) with treatment in the two clinical trials (Fig. 1G), whereas most of the patients with high *RasGRP1* expression (88 of 93, or 95%) went into remission followed by a relapse or into complete continuous remission.

Rasgrp1 integrations are highly prevalent in mouse T-ALLs generated by retroviral insertional mutagenesis

We next examined two independent mouse leukemia screens and identified *Rasgrp1* as a CIS. In the first retroviral insertion mutagenesis (RIM) screen, T lineage leukemias were induced by SL3-3 mouse leukemia virus insertions in BALB/c mice. Fathers of SL3-3–infected mice were treated with the *N*-ethyl-*N*-nitrosourea (ENU) mutagen (*29*) to generate random mutations in the genome before being infected with leukemia virus. In 237 leukemias, CIS were found within ~159 kb of *Rasgrp1*, a frequency similar to that of the leukemia-associated oncogenes *Evi5*, *Notch1*, and *pvt1* (Fig. 2A). As an example, *Notch1* expression becomes activated by both retroviral CIS and point mutations in mouse T-ALL (*30*), and *Notch1* is a very common target of somatic mutation in human T-ALL (*31*). In contrast to the abundant SL3-3 CIS in *Rasgrp1*, we found only one insertion each in *Rasgrp4* and *Rasgrf1*, but none in the genes encoding the other five RasGEFs from a total of 6234 mapped integrations (Fig. 2B). Despite our predicted effects of reduced RasGAP activity or abundance leading to increased Ras activation (Fig. 1), we observed very few insertions in genes encoding RasGAPs (Fig. 2C). Consistent with this finding, inactivation of the RasGAP-encoding *NF1* occurs infrequently in pediatric T-ALL (*32*), although these results may reflect the lower statistical chance of interrupting the coding region of the genes of inhibitors such as RasGAP proteins. Most of the *Rasgrp1* insertions mapped to the promoter region, some to intron 1, and one single SL3-3 tag marked the 3′ untranslated region (Fig. 2D and figs. S2, A and B, and S3).

CIS in *Rasgrp1* have been reported in other RIM screens of smaller scale (see fig. S2B for CIS positions) (*33*–*35*). Transgenic overexpression of *Rasgrp1* causes thymic lymphomas in mice (*36*), and retroviral overexpression of *Rasgrp1* in bone marrow cells followed by transplantation into sublethally irradiated recipient mice results in T-ALL with $CD3^{low}CD4^{+}CD8^{+}Thy1^{+}$

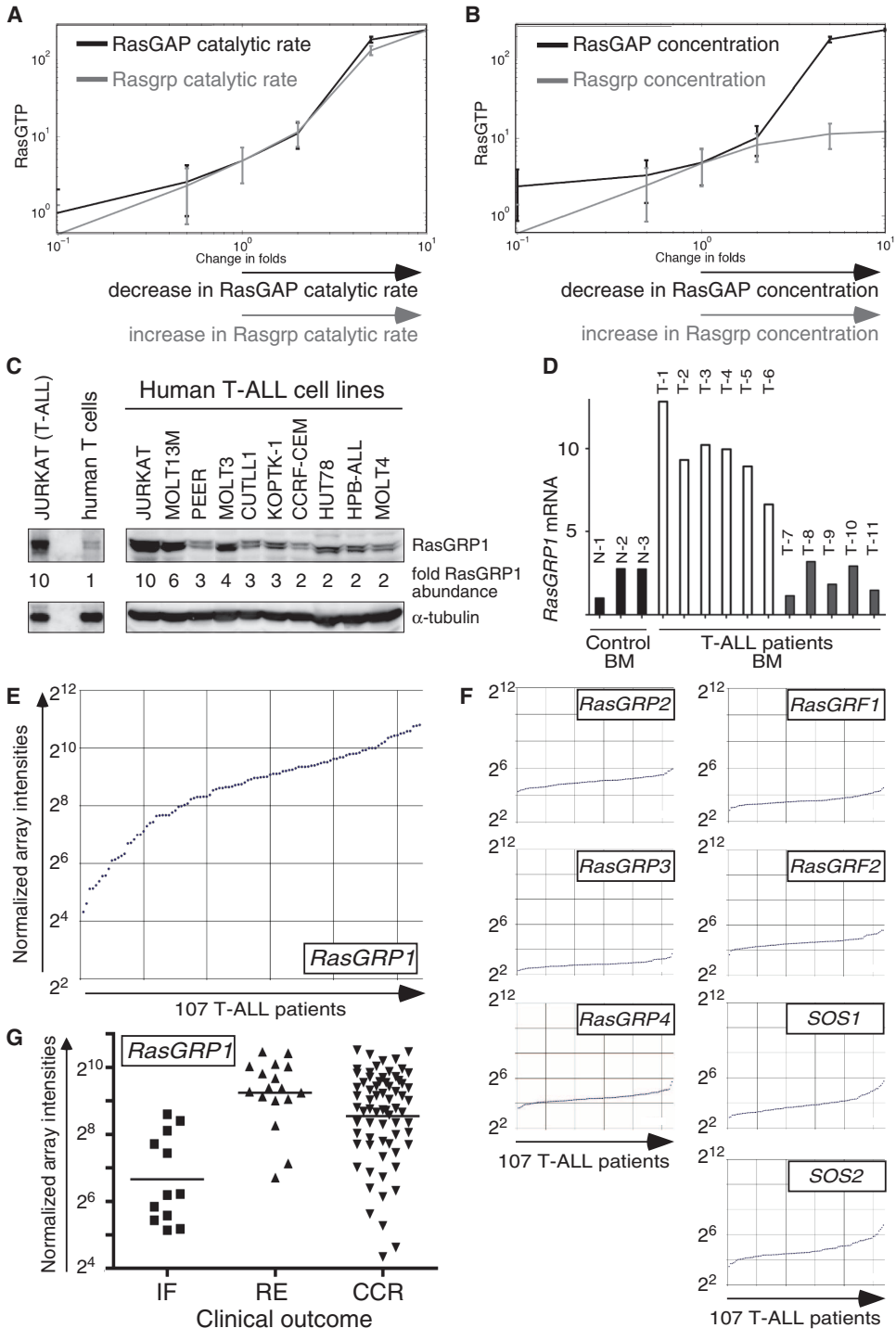

Fig. 1. Increased RasGRP1 abundance is a common feature of human T-ALL. (**A** and **B**) In silico prediction of the effect of changing (A) the catalytic rates and (B) the concentrations of RasGAP and RasGRP1 on Ras activation. The SOS concentration was set at a basal amount (5 simulation concentration units). Each data point reported represents the average of 10,000 simulation trajectories at 200 simulation time units. The error bars indicate SDs, which measure cell-to-cell variability. Qualitatively similar results were observed when the SOS concentration was increased from 5 to 15 (see fig. S1, B and C). (**C**) Western blotting analysis of RasGRP1 protein abundance in a panel of established human T-ALL lines with abundance in normal T cells arbitrarily set at 1. Data are representative of three independent experiments. (**D**) Real-time RT-PCR analysis of *RasGRP1* expression in bone marrow samples of pediatric T-ALL patients (T; 18 years or younger) or healthy donors (N). RasGRP1 mRNA abundances were normalized to those of *GAPDH*, and *RasGRP1* expression was arbitrarily set to 1.0 in the sample from healthy donor N-1. (**E** and **F**) Standard Affymetrix analyses were used to generate and normalize signal intensities of *RasGRP1* mRNA abundances in samples from 107 pediatric patients enrolled in the COG studies 9900/9404 and AALL03B1/AALL0434. Analyses of robust multichip average (RMA)–normalized data were plotted and indicated a statistically significant 128-fold range in the abundance of *RasGRP1* mRNA, but not of any other RasGEF mRNA. (**G**) *RasGRP1* mRNA abundance plotted as a function of clinical outcome. Low *RasGRP1* mRNA abundance correlated with induction failure (IF). Patients with greater *RasGRP1* mRNA abundance in general went into remission followed by relapse (RE) or displayed complete continuous remission (CCR).

leukemic T cells (*28*), but the mechanisms by which *Rasgrp1* contributes to leukemogenesis have not been explored. In normal thymocytes, *Rasgrp1* mRNA amounts are dynamic during development (*37*) and are reduced in response to T cell receptor (TCR) stimulation (*38*). To investigate the effect of CIS in *Rasgrp1*, we first generated clonal T-ALL cell lines from primary leukemia tumors and subsequently derived daughter cell lines in which we targeted *Rasgrp1* or *Sos1* expression with lentiviruses expressing specific short hairpin RNAs (shRNAs). This panel of cells also included two T-ALL cell lines (numbers 55 and 98) that had SL3-3 integrations in loci other than *Rasgrp1*, and displayed similar amounts of the TCR, CD4, and CD8 developmental markers to those of T-ALL cell lines with *Rasgrp1* insertions (Fig. 2E and fig. S3, B and C). The SL3-3 *Rasgrp1* CIS T-ALL cell lines demonstrated increased amounts of *Rasgrp1* mRNA in comparison to those of the SL3-3 T-ALL 98 cell line (Fig. 2E and fig.

A

6234 insertion sites identified from 2199 T cell lymphomas

1.	*Evi5*	253 insertions
2.	*Notch1*	253 insertions
3.	*pvt1*	243 insertions
4.	*Rasgrp1*	237 insertions

B

Rasgrp2	0 insertions
Rasgrp3	0 insertions
Rasgrp4	1 insertion
SOS1	0 insertions
SOS2	0 insertions
Rasgrf1	1 insertion
Rasgrf2	0 insertions

C

DAB2IP	0 insertions
IQGAP1	0 insertions
IQGAP2	0 insertions
NF1	0 insertions
Plexin-B1	0 insertions
Plexin-C1	0 insertions
Rap1GAP	0 insertions
Rasa1	0 insertions
Rasa2	1 insertion
Rasa3	1 insertion
Rasa4	0 insertions
RASAL1	0 insertions
RASAL2	0 insertions
Sipa1	0 insertions
Syngap1	0 insertions
TSC1	0 insertions
TSC2	0 insertions

D

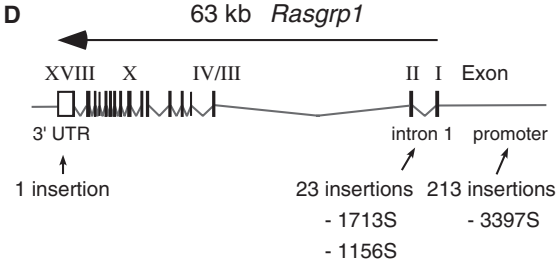

E

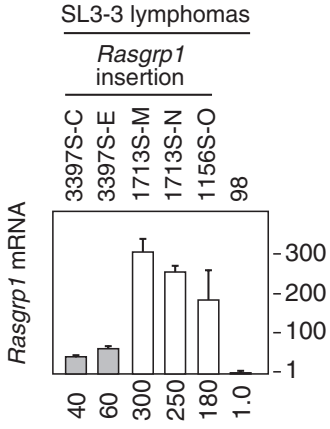

Fig. 2. Retroviral insertions in the *Rasgrp1* locus are frequent in mouse T-ALL and result in enhanced *Rasgrp1* expression, whereas CIS in the genes encoding other RasGEFs or RasGAPs are rare. (**A**) Overview of the four most frequent insertion sites as determined by our in vivo BALB/c mouse screen. Fathers of mice injected with SL3-3 were mutagenized with ENU. (**B**) Frequency of SL3-3 CIS in the other seven RasGEF-encoding genes. (**C**) Numbers of SL3-3 insertions in 17 RasGAP-encoding genes. (**D**) Genomic locations of SL3-3 insertions in *Rasgrp1*. See figs. S2 and S3A for a detailed map of the insertions in *Rasgrp1*. (**E**) Increased *Rasgrp1* mRNA abundance in clonal SL3-3 lymphoma cell lines that were generated from the primary tumor 3397S, which had an SL3-3 insertion in the *Rasgrp1* promoter, as well as from tumors 1713S and 1156S, which had insertions in intron 1. The abundances of *Rasgrp1* mRNA in these lines were compared to that in the control T-ALL 98 cell line in which *Rasgrp1* mRNA abundance, as determined by real-time RT-PCR, was arbitrarily set at 1.0. Data are means and SEs from three independent experiments.

S3C). Together, these data demonstrate that retroviral CIS in *Rasgrp1* are uniquely frequent and result in dysregulated, enhanced *Rasgrp1* expression in mouse T-ALL.

Dysregulated *Rasgrp1* and *K-Ras*^{G12D} are mutually exclusive and cause distinct Ras activation as well as in vitro and in vivo proliferative patterns

We also observed *Rasgrp1* CIS in three of six T-ALLs in a second, smaller screen with MOL4070 retrovirus in wild-type C57BL/6/129SvJ mice, and we generated the C6 and C7 MOL4070 T-ALL cell lines. In contrast, 46 T-ALLs from the same MOL4070 RIM screen performed in mice with a genetic *K-Ras*^{G12D} mutation (*39*) did not harbor any *Rasgrp1* CIS, suggesting that oncogenic *K-Ras*^{G12D} mutations and insertions in *Rasgrp1* do not have additive effects in leukemogenesis.

Similar to the regulation of its mRNA, Rasgrp1 protein abundance is also regulated in a dynamic manner and decreases after the maturation of normal developing T cells (*40*, *41*). In agreement with the effects of CIS in *Rasgrp1* on its mRNA abundance, Rasgrp1 protein amounts were about four- to sixfold greater in all murine T-ALL with *Rasgrp1* CIS than in normal total thymocytes and lymph node T cells (Fig. 3A and fig. S3D), differences that are similar in magnitude to what we observed for human T-ALL lines (Fig. 1C). In contrast, Rasgrp1 protein was low in abundance in the T-ALL 55 and 98 cell lines, which had similar amounts of the markers TCR, CD4, and CD8, but had other CIS, not in *Rasgrp1* (fig. S3D). Rasgrp1 protein was practically undetectable in all six *K-Ras*^{G12D} T-ALL lines (Fig. 3A and fig. S3D). Five of these six *K-Ras*^{G12D} T-ALL lines had undetectable cell-surface TCR, indicative of these cell lines being at an earlier developmental stage than the other cell lines examined. This mirrors the human disease with *RAS* mutations and the early developmental stage of ETP T-ALL (*21*). It is possible that Rasgrp1 protein is undetectable in ETP T-ALL types (*21*) because, normally, early thymocyte subsets express low amounts of Rasgrp1 (*40*, *41*). Thus, our panel of murine T-ALL lines spans different developmental stages, similar to what has been reported for human T-ALL lines (*27*) and in agreement with the apparent variation in the developmental stages of primary T-ALL in patients (*4*, *7*, *8*, *10*–*12*).

Our panel of cell lines from SL3-3–induced leukemias with *Rasgrp1* integrations and cell lines from MOL4070-induced *K-Ras*^{G12D} mutant and wild-type leukemias enabled us to directly compare the biochemical effects of dysregulated Rasgrp1 and oncogenic *K-Ras*^{G12D} expression on Ras, as well as explore potential differences in the underlying molecular mechanisms of the associated T lineage leukemogenesis. We first examined the amounts of RasGTP in these clonal T-ALL lines under basal, serum-free conditions. As anticipated from their impaired GTPase function (*17*), all *K-Ras*^{G12D} T-ALL cell lines had increased amounts of GTP-loaded Ras in the basal state compared to that of *Rasgrp1* T-ALL cell lines (Fig. 3A). In contrast, *Rasgrp1* T-ALL lines displayed only low amounts of RasGTP under basal conditions, which were further reduced in a T-ALL daughter line in which Rasgrp1 abundance was reduced by 57% by Rasgrp1-specific shRNA (fig. S3E).

Paradoxically, strong oncogenic signals can trigger cell cycle arrest and promote apoptosis, and the p53–p21 CDK-interacting protein (p21^{CIP}) arrest pathway plays a central role in this response (*42*, *43*). This pathway can be induced by robust signals from *Myc* or *Ras* oncogenes and by DNA damage, and it is often disrupted in cancer (*42*, *43*). On the basis of the different extents of basal Ras signaling in our T-ALLs, we hypothesized that *K-Ras*^{G12D} and *Rasgrp1* T-ALL might show distinct patterns of cell cycle arrest. Indeed, the phosphorylation of p53 and the production of

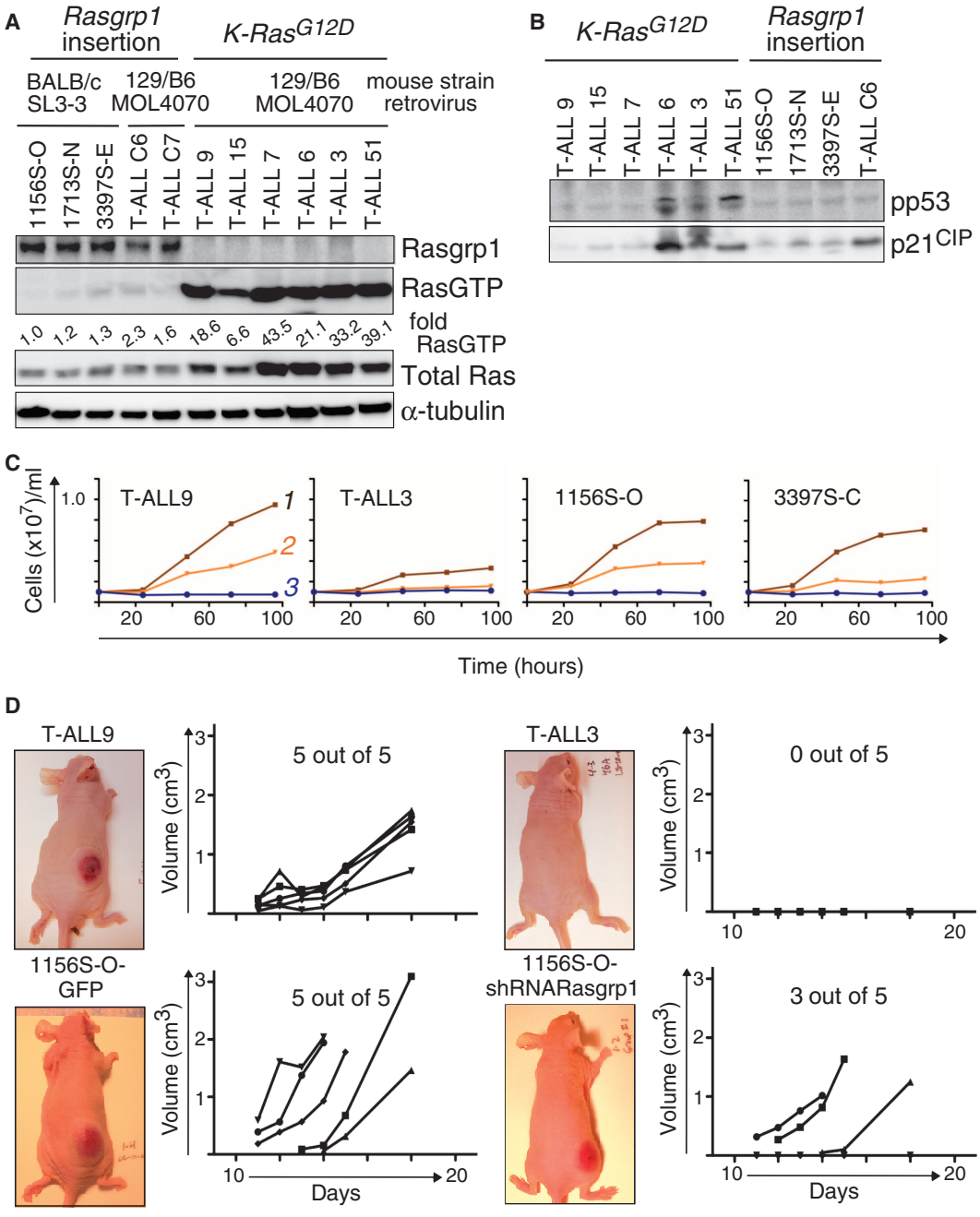

Fig. 3. *Rasgrp1* and *K-Ras*^{G12D} oncogenes induce Ras activation to different extents and drive proliferation in distinct manners. (**A**) Analysis of basal RasGTP and Rasgrp1 abundances in the indicated *Rasgrp1* and *K-Ras*^{G12D} T-ALL lines. Only 20% of the RasGTP pull-down material was loaded for all *K-Ras*^{G12D} lines to remain in the dynamic range for quantification by Western blotting analysis, which was later corrected by a factor of 5. The abundance of RasGTP in 1156S-O cells was arbitrarily set to 1.0 by normalizing to the abundance of α-tubulin protein. (**B**) Analysis of the p53-p21^{CIP} cell cycle arrest pathway in the indicated T-ALL lines. Phosphorylated p53 (pp53) was measured 6 hours after seeding the cells in culture medium, whereas p21 abundance was determined after 24 hours. Protein loading controls and positive controls for cell cycle arrest triggered by doxorubicin are presented in fig. S4. (**C**) In vitro proliferation assays were performed with cells incubated over a 100-hour period with complete medium (condition 1, brown), medium with 20% of normal serum content (condition 2, orange), or complete medium with doxorubicin (condition 3, blue). Cells were seeded at 10^6/ml, and live cells were counted over the period. A combination of IL-2, IL-7, and IL-9 was added to the culture medium to ensure sufficient growth factor presence. For additional growth curves and measurement of proliferation in the absence of cytokines, see figs. S4 and S5. Data in (A) to (C) are representative of three or more experiments. (**D**) Analysis of the in vivo proliferative potential of *K-Ras*^{G12D} and *Rasgrp1* T-ALL cells. T-ALL cells (1×10^5) were injected subcutaneously into nude mice, and proliferation was determined by measuring tumor volume (in cm^3) over time. For additional images and growth curves, see fig. S6. Each curve is derived from a single mouse.

the p53 target $p21^{CIP}$ were constitutively induced in the *K-Ras*^{G12D} T-ALL cell lines 6, 3, and 51 (Fig. 3B). In a second group of *K-Ras*^{G12D} T-ALL cell lines (which included lines 9, 15, and 7), we did not observe triggering of the expected p53-$p21^{CIP}$ arrest pathway. In contrast, the abundances of phosphorylated p53 and of $p21^{CIP}$ were very modest in all *Rasgrp1* T-ALL lines that had low amounts of RasGTP under basal conditions (Fig. 3B and fig. S4). As a positive control, we showed that the p53-$p21^{CIP}$ pathway was stimulated by doxorubicin-induced DNA damage in T-ALLs (fig. S4, A and B).

These distinct biochemical features were reflected in different cellular proliferative patterns in vitro. The *K-Ras*^{G12D} T-ALL cell lines 6, 3, and 51 underwent apoptosis and cell death in the absence of exogenous growth factors, as measured by staining with annexin V– or with annexin V and propidium iodide (PI) (fig. S4C). These same cell lines showed modest proliferation in vitro that depended on the presence of IL-2, IL-7, and IL-9 in the culture medium (Fig. 3C and fig. S5). The *K-Ras*^{G12D} T-ALL cell lines 9, 15, and 7 and all of the *Rasgrp1* T-ALL lines showed little apoptosis and cell death (fig. S4, D and E), which resulted in exponential cellular proliferation in vitro even in the absence of cytokines or when the amount of fetal calf serum in the medium was reduced (Fig. 3C and fig. S5).

To investigate the basal proliferative potential of these cell lines in vivo, we transplanted nude mice subcutaneously with T-ALLs because this region of the mouse represents a nonhematopoietic site that typically lacks abundant growth factors. Nude mice are also immunocompromised, which enabled us to make a direct side-by-side comparison of T-ALL lines derived from mice with different genetic backgrounds (BALB/c and C57BL/6/129). In agreement with our earlier in vitro data, we found that mice injected with the *K-Ras*^{G12D} T-ALL 3 and 6 cell lines never developed tumors subcutaneously, whereas all eight mice that received the *K-Ras*^{G12D} T-ALL 9 or 15 cell lines developed palpable tumors after 12 to 14 days (Fig. 3D and fig. S6). Eight of the 10 mice that were injected with two independent *Rasgrp1* T-ALL cell lines (1156S-O and 1713S-N) also developed tumors (Fig. 3D and fig. S6). We reduced the abundance of Rasgrp1 in 1156S-O cells by 57% (by infecting them with retrovirus expressing Rasgrp1-specific shRNA) and found that this decreased the incidence of tumors in transplanted mice compared to mice transplanted with 1156S-O cells expressing green fluorescent protein (GFP) (Fig. 3D and fig. S6). Thus, increased Rasgrp1 abundance contributed to T-ALL cell proliferation and tumor development in vivo. We did not observe the antiproliferative effects of Rasgrp1-specific shRNA in T-ALLs in vitro at the 96-hour time point (fig. S5), which indicated that the in vivo assays were more stringent tests of growth potential.

Reduced Rasgrp1 abundance retards T-ALL development in hematopoietic organs

Cytokines play an important role in leukemogenesis and leukemia progression, and transgenic overexpression of IL-7 or IL-9 promotes these processes in mouse models (*44*, *45*). These studies were further substantiated by the identification of activating mutations in the gene encoding IL-7R in T-ALL patients (*21*, *22*). Cytokine receptors of the common γ-chain family relay signals through the common γ chain to promote the proliferation and survival of T-ALLs in response to stimulation by their cytokines (*46*, *47*). Part of this cytokine receptor response occurs through the JAK–signal transducer and activator of transcription (STAT) axis (*48*), which can be involved in T-ALL patients (*49*), although other pathways could also play a role. To first test whether our T-ALL cell lines were subject to autocrine cytokine stimulation, we examined the expression of *IL2*, *IL7*, and *IL9* in our clonal lines that were grown in log phase in tissue culture. The *K-Ras*^{G12D} T-ALL 3 and 6 cell lines, which had impaired proliferation (Fig. 3), had relatively large amounts of *IL2* and *IL7* mRNAs and small amounts of *IL9* mRNA, as measured by real-time RT-PCR analysis, with the amounts of *IL9* mRNA slightly increased compared to those of activated $CD4^+$ T cells (Fig. 4, A and B). In contrast, the amounts of these cytokine mRNAs were negligible in all other T-ALL lines (Fig. 4A) in vitro and after being transplanted subcutaneously into mice, and were not affected by knockdown of Rasgrp1 (Fig. 4C), indicating that autocrine stimulation of cells through IL-2, IL-7, or IL-9 production did not play a substantial role in the proliferative responses of our T-ALL lines.

We reasoned that cell proliferation could be stimulated by cytokines produced by stromal cells. To test this hypothesis, we injected *Rasgrp1* T-ALL lines into the mouse circulatory system. Similar to what is observed in T-ALL patients, *Rasgrp1* T-ALL cell lines preferentially proliferated in the hematopoietic organs of injected mice. Two weeks after the introduction of 4000 cells into recipient mice, we observed large percentages of GFP-marked 1156S-O and 3397S-E T-ALL cell lines in the bone marrow and livers (Fig. 4D and fig. S7B). Knocking down Rasgrp1 in 1156S-O T-ALL cells by 57% with shRNA before being injected into mice (Fig. 5B) significantly reduced the frequency of GFP^+ cells in the bone marrow and liver compared to that of control mice injected with cells in which Rasgrp1 had not been knocked down (Fig. 4D, $P = 0.011$ and $P = 0.007$, respectively). Knockdown of Rasgrp1 by 37% in 3397S-E T-ALL cells resulted in a similar trend in the bone marrow, although autofluorescence interfered with the lower amounts of GFP in this T-ALL line, particularly hindering the analysis in the liver (fig. S7, A and B). Knockdown of Rasgrp1 was relatively stable in vivo and extended the mean survival times of mice transplanted with 1156S-O T-ALL cells (fig. S7, C and D).

Histological examination of blood smears indicated an increased proportion of circulating blasts in the peripheral blood of mice injected with 1156S-O T-ALL cells compared to that of mice injected with 1156S-O cells in which Rasgrp1 was knocked down by shRNA (Fig. 4E). Similarly, hematoxylin and eosin (H&E) and Rasgrp1 staining indicated a high T-ALL burden in the bone marrow and livers of these mice. Morphologically homogeneous T-ALL blasts that were positive for Rasgrp1 in the bone marrow resulted in a concomitant loss of cellular heterogeneity in the bone marrow (for example, notice the decrease in megakaryocytes). Similarly, T-ALL cells also efficiently proliferated in the liver and caused destruction of the normal hepatocyte network (Fig. 4F). This pathology was substantially reduced when Rasgrp1 was knocked down in the injected cells (Fig. 4F). These results demonstrate that reducing Rasgrp1 abundance, even only partially, retards tumor growth in vivo, suggesting that Rasgrp1 might be an attractive target molecule for future cancer therapy.

Increased Rasgrp1 abundance enhances the responsiveness of cells to diacylglycerol stimulation

Basal amounts of RasGTP are only modestly increased in *Rasgrp1* T-ALL cell lines; however, all of these cell lines exhibit substantial proliferative responses in vitro. In normal lymphocytes, the membrane recruitment and activation of Rasgrp1 depends on diacylglycerol (DAG), a second messenger that is produced by phospholipase Cγ (PLC-γ) (*50*). To test whether *Rasgrp1* T-ALL lines were responsive to DAG, we stimulated them with phorbol 12-myristate 13-acetate (PMA), a synthetic version of DAG, and monitored the activation of Ras. PMA most stimulated the production of RasGTP when Rasgrp1 abundance was high. Induction of RasGTP was more modest in a control T-ALL 55 cell line without CIS in Ras-related genes coming from the same SL3-3 screen, and RasGTP was also reduced in T-ALL lines expressing Rasgrp1-specific shRNA (Fig. 5, A to C). The amount of Rasgrp1 in all of the T-ALL cell lines also directly correlated with the extent of phosphorylation (and activation)

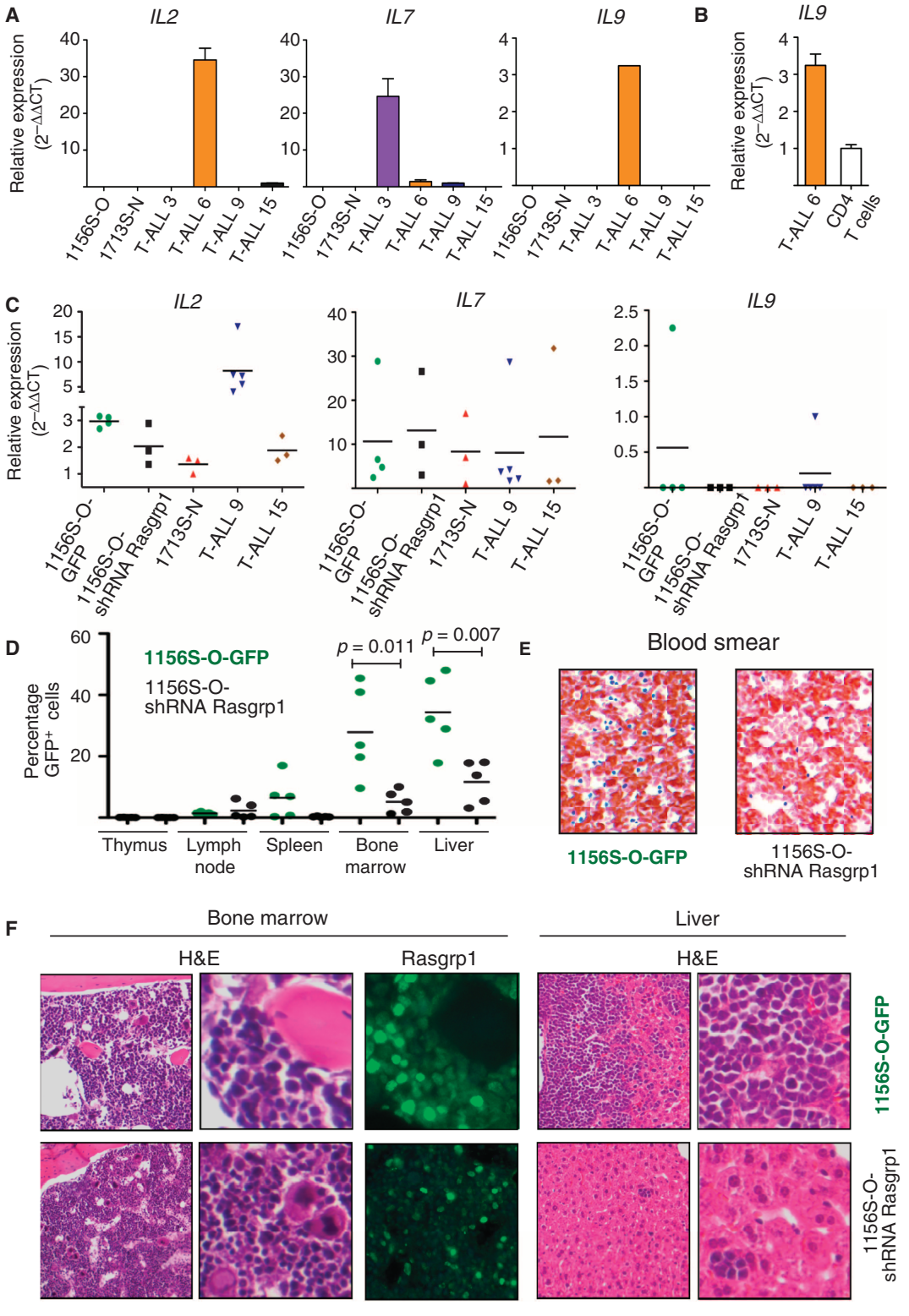

Fig. 4. Potential role of cytokine signaling in *Rasgrp1* T-ALL. (**A** and **B**) We used real-time RT-PCR analysis to measure the abundances of *IL2*, *IL7*, and *IL9* mRNAs in the indicated T-ALL cell lines that were maintained in an exponential log phase in tissue culture in complete medium. In (B), $CD4^+$ T cells that were activated with PMA and ionomycin were used as a positive control for *IL9* expression. Relative mRNA abundances are plotted as the $\log_2$ of the inverse function of the ΔC_T (difference in cycles), normalized to the abundance of *GAPDH* mRNA. Data are means and SEs from three independent experiments. (**C**) Real-time RT-PCR analysis of cytokine mRNAs from T-ALL that proliferated subcutaneously in nude mice. Means (horizontal bars) and abundances in individual tumors (symbols) are plotted. (**D**) Quantification of the frequency of GFP-containing (GFP^+) T-ALL cells in individual mouse organs as determined by flow cytometric analysis. Five mice of each group were injected with 4000 T-ALL cells and were analyzed 14 days later. See fig. S7 for results with the 3397 T-ALL cell line. Data are representative of two independent experiments, and each dot represents an individual mouse. Note the statistically significant reduction in GFP^+ cells in the bone marrow and liver when Rasgrp1 was knocked down with shRNA ($P < 0.05$). (**E** and **F**) Histological analysis of T-ALL. (E) H&E staining of blood smears at 17 days after subcutaneous injection for GFP-labeled 1156S-O-GFP T-ALL demonstrated a high frequency of T-ALL cells circulating in the blood (blue cells). Injection of 20,000 1156S-O-shRNA Rasgrp1 cells resulted in fewer T-ALL in the blood, monitored at 22 days after injection. (F) Bone marrow and liver sections from the mice in (D) were analyzed for bone marrow and liver morphology, as well as the presence of T-ALL blasts and Rasgrp1 abundance, by H&E and Rasgrp1 staining. Representative images are shown from three mice for each condition tested.

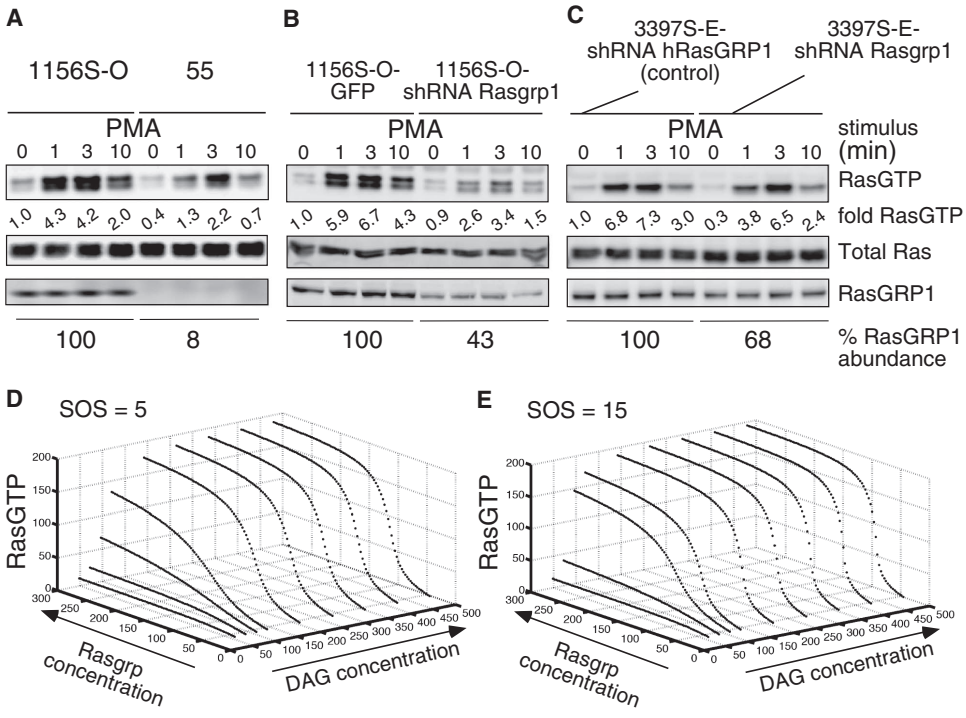

Fig. 5. DAG has the potential to activate Rasgrp1 and stimulate increased RasGTP production in T-ALL. (A to C) PMA induced rapid and enhanced Ras activation in a Rasgrp1-dependent manner. RasGTP pull-down assays and analysis of Rasgrp1 abundance in the indicated T-ALL cell lines that were serum-starved and then stimulated with PMA (25 ng/ml) for the indicated times. The amount of RasGTP in resting 1156S-O T-ALL was arbitrarily set at 1.0. For downstream ERK activation patterns, see fig. S8. Data in (A) to (C) are representative of three or more experiments. (D and E) Deterministic steady-state amount of RasGTP modeled as a function of DAG and Rasgrp concentrations at different low amounts of Sos. The amounts of Sos were arbitrarily set at 5 and 15 activation units.

of the mitogen-activated protein kinase (MAPK) extracellular signal–regulated kinase (ERK), which is downstream of the RasGTP–Raf kinase–MEK (mitogen-activated or extracellular signal–regulated protein kinase kinase) pathway (fig. S8, A to G).

Because DAG amounts and turnover play a role in controlling Rasgrp-induced Ras activation in normal lymphocytes (*51*), we used our computational model (Fig. 1) to explore the effects of incrementally increasing the amounts of Rasgrp and DAG in T-ALL. Jointly varying the concentrations of both components, while keeping SOS at a fixed amount of 5 or 15, predicted a strong cooperation between the increased amounts of Rasgrp and of the second messenger DAG in the simulations (Fig. 5, D and E). Note that both concentrations of SOS resulted in sigmoid curves for RasGTP abundances as a function of DAG and Rasgrp concentrations, predicting that there is a threshold phenomenon for DAG-Rasgrp-Ras signaling in T-ALL. These simulations led us to suggest the hypothesis that sufficient amounts of basal DAG or newly generated DAG in response to upstream receptor signals might be required for the effect of increased Rasgrp1 abundance in T-ALL.

The amount of Rasgrp1, but not of Sos1, determines the strength of the cytokine-Ras response

In normal lymphocytes, RasGRP1 and SOS1 are recruited to the plasma membrane and cooperate to activate Ras when the TCR or B cell receptor (BCR) is stimulated; however, RasGRP1 is dominant over Sos1 (*52*). The dominant effect of RasGRP1 can be explained by the fact that the RasGRP1-generated RasGTP not only transmits signals to its downstream effectors, such as the kinase Raf, but also exponentially enhances the GEF activity of SOS by binding to SOS and allosterically activating SOS so that much more RasGTP is produced (*24*, *52*, *53*). Thus, the allosteric activation of SOS is facilitated by RasGRP1. To predict how receptor signals might influence Ras activation in our T-ALL, we incorporated receptor input into our computational models, following Riese *et al.* (*51*), and determined RasGTP abundance as a function of increasing concentrations of Rasgrp and increasing receptor signal input at simulation time units of t = 5 and 15 (Fig. 6, A and B). The resultant sigmoid curves indicated that once Rasgrp concentrations surpass a certain threshold, in these particular cases for arbitrary amounts of Rasgrp greater than ~100 simulation concentration units, RasGTP is generated very efficiently in the context of receptor stimulation. Moreover, and conversely, it was predicted that when the amount of Rasgrp drops below this threshold (for example, when Rasgrp = 50 or 75 units; Fig. 6, A and B), RasGTP generation will be very limited, even when signal input is substantial.

To test these predictions and to mimic the exposure of T-ALL to physiological stimuli such as growth factors produced by stromal cells, we stimulated our cell lines with a cocktail of the cytokines IL-2, IL-7, and IL-9. Such stimulation resulted in strong RasGTP production in *Rasgrp1* T-ALL (Fig. 6, C to E). The shRNA-dependent knockdown of Rasgrp1 by 55 and 48% in 1156S-O and T-ALL C6 cells, respectively, resulted in markedly reduced cytokine-induced amounts of RasGTP compared to those in control cells (Fig. 6, D and E), suggesting that Rasgrp1 responds to a cytokine receptor–induced signaling pathway. Note that these cytokine-induced Rasgrp1-RasGTP responses were transient and that the amounts of RasGTP generated were lower than the basal amounts of RasGTP in the *K-Ras*^{G12D} T-ALL 3 line. In addition, a combination of IL-2, IL-7, and IL-9 enhanced the already increased amount of RasGTP in the *K-Ras*^{G12D} T-ALL 3 cell line (Fig. 6C).

Sos1 is found in our T-ALL lines (Fig. 6, C to E) and is presumably recruited to stimulated cytokine receptors through the adaptor molecules Shc and Grb2, which link the receptors to SOS, so it can activate membrane-bound Ras (*54*). Our previous work suggested that Rasgrp transduces essential low-level receptor signals to Ras in an analog manner until a threshold of receptor input is reached, at which point the character of the Ras activation is altered because SOS is also engaged, which results in digital Ras signals or a sharp threshold that separates weaker signaling from strong signaling (*24*, *55*). This does not mean that Rasgrp alone cannot generate strong Ras signals. For example, here we predicted (Fig. 1) that for T-ALL, complete removal of SOS (SOS = 0) still enabled the generation of substantial amounts of RasGTP, provided that the simulation concentration units of Rasgrp1 were sufficiently high (>~100). However,

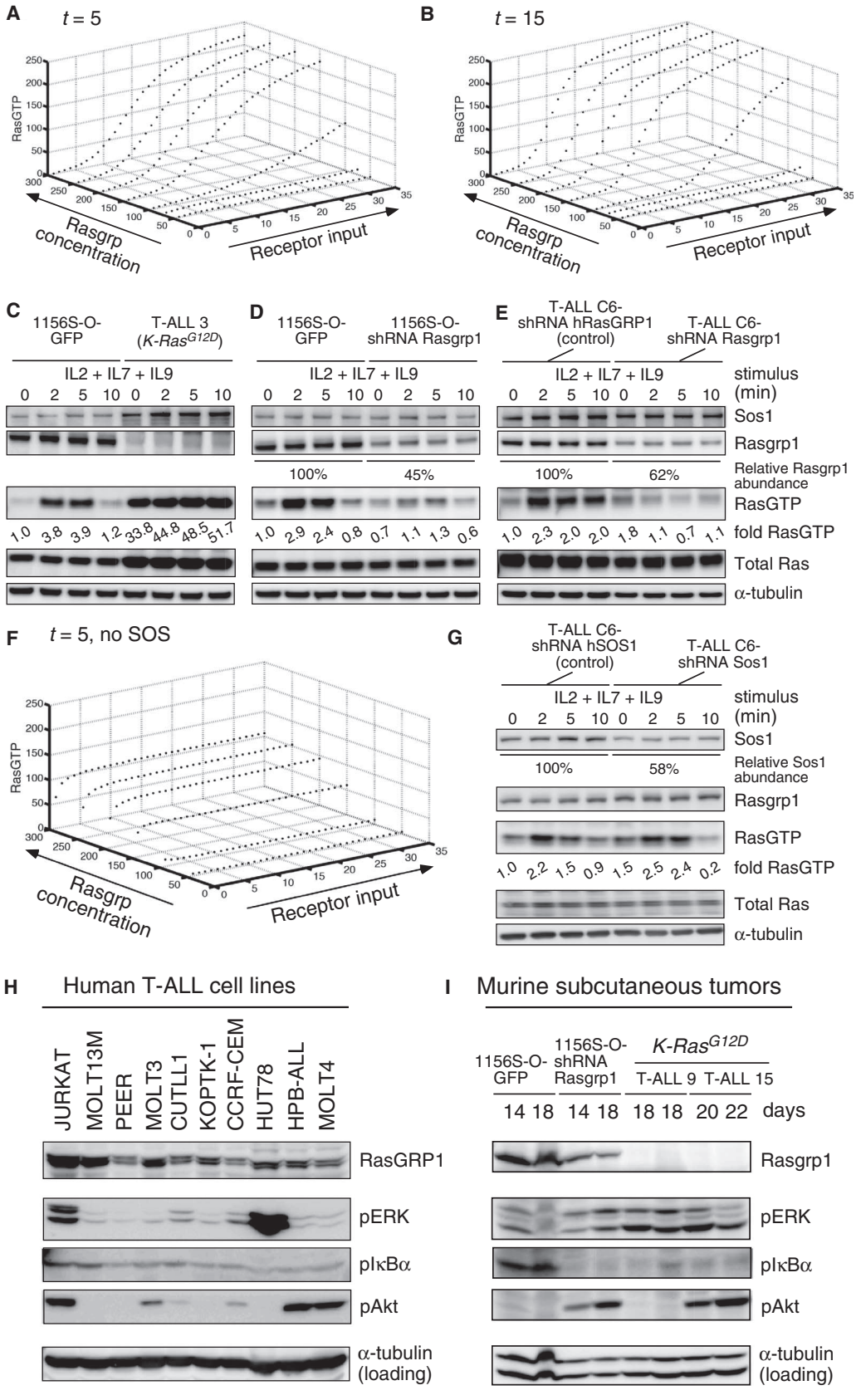

Fig. 6. The abundance of Rasgrp1, but not of Sos1, is important for cytokine-induced Ras activation in T-ALL. (**A** and **B**) RasGTP production as a function of Rasgrp concentration and receptor input at (A) $t = 5$ simulation time units and (B) $t = 15$ simulation time units. Each data point represents the average of 10,000 simulation trajectories. (**C** to **E**) Cytokine stimulation induces strong, but transient, Ras activation in the *Rasgrp1* 1156S-O and C6 T-ALL cell lines and enhanced production of RasGTP in the *K-Ras*^{G12D} T-ALL 3 cell line. Lentivirally expressed shRNA led to Rasgrp1 knockdown in 1156S-O and T-ALL C6 by 55 and 38%, respectively, which resulted in decreases in cytokine-induced RasGTP abundance. Note that Sos1 abundance was unchanged. (**F**) Computational predictions of receptor-induced Ras activation as described in (A) and (B) but in which all input from SOS has been removed. (**G**) In contrast to the substantial decrease in cytokine-induced Ras activation in T-ALL C6 after a 38% reduction in Rasgrp1 abundance, a reduction in Sos1 abundance by 42% in the same C6 T-ALL cell line had no substantial effect on RasGTP generation. As a specificity control for the shRNA for murine Sos1, C6 T-ALL cells were transduced with lentivirus expressing shRNA specific for human SOS1. Data in (C) to (E) and (G) are representative of three independent experiments. (**H**) Patterns of phosphorylation of ERK, Akt, and IκBα in unstimulated human T-ALL lines. Data are representative of two experiments. (**I**) Pathway analysis of individual subcutaneous T-ALL tumors (from experiments in Fig. 3D and fig. S6). The patterns of phosphorylation of ERK, Akt, and IκB demonstrate complex heterogeneity in *K-Ras*^{G12D} T-ALL as well as plasticity in *Rasgrp1* T-ALL. Data are representative of three experiments.

the exponential pattern of RasGTP generation was predicted to be absent without SOS (Fig. 6F), which is consistent with our past experimental results (*24*, *55*). We tested the efficacy of various Sos1-targeting shRNA constructs. Unfortunately, none of these resulted in a complete knockdown of Sos1, and therefore, the effect of the predicted loss of exponential Ras activation (Fig. 6F) is likely best tested through genetic Sos1-deleting models that will have to be generated in the future. However, reduction of Sos1 abundance by 42%, which was similar in magnitude to the knockdown of Rasgrp1 observed earlier (Fig. 6, D and E), did not affect the strength of cytokine-induced Ras activation in the T-ALL C6 cell line (Fig. 6G). Thus, cytokine-induced Ras activation in *Rasgrp1* T-ALL is more sensitive to decreases in Rasgrp1 abundance than to decreases in Sos1 abundance.

Gene expression profiling and cell-surface marker profiling have not yet led to a successful stratification of T-ALL (*4*, *7*, *8*, *10*–*12*), which contrasts with the successful classification of diffuse large B cell lymphoma (*9*). Here, we made a start to explore the biochemical stratification of T-ALL. The heterogeneity in cytogenetic abnormalities (*4*–*6*) and the differences in developmental stages of T-ALL (*7*) are likely to increase the biochemical diversity and may complicate the identification of a universal molecular target for clinical intervention. Indeed, the limited cell proliferation assays that have been reported with T-ALL patient cells demonstrate a wide range of responses to stimulation with various cytokines in vitro (*47*), suggesting a high degree of heterogeneity in the signals transmitted through the cytokine receptor pathways.

RasGTP signals to multiple effector kinase pathways, such as the Raf-MEK-ERK and the phosphoinositide 3-kinase (PI3K)–Akt–mammalian target of rapamycin (mTOR)–S6 kinase pathways that stimulate cell proliferation and survival (*54*, *56*). Directly targeting oncogenic Ras proteins is difficult, because it would involve restoring the impaired GTPase function of Ras and it has not proven feasible to date (*57*). As a result, considerable effort is ongoing to interfere with molecules downstream of Ras in clinical settings, such as MEK or PI3Ks (*56*), as potential cancer therapies. Consistent with the reported heterogeneous proliferative responses (*47*), we observed heterogeneous patterns of phosphorylation of ERK and Akt in our panel of human T-ALL cell lines that did not correlate with RasGRP1 abundance (Fig. 6H). Variability in activity through the PI3K-Akt pathway in some of these T-ALL lines was previously noted (*26*, *58*). Similarly, our murine T-ALL lines that proliferated after subcutaneous injection in vivo also exhibited heterogeneous activation of these effector kinase pathways. Analysis of cells from two tumors removed from mice independently injected with the *K-Ras*^{G12D} T-ALL 15 cell line demonstrated that they exhibited Akt signaling, whereas cells from two T-ALL 9–derived tumors with the same genetic *K-Ras*^{G12D} lesion did not (Fig. 6I). Because cells from all eight tumors derived from the *K-Ras*^{G12D} T-ALL 15 and 9 cell lines proliferated to similar extents (fig. S6), we conclude that the T-ALL 9 cells must have other signals engaged that have a biological function similar to that of Akt signaling in T-ALL 15 cells. Moreover, we found that clonal 1156S-O *Rasgrp1* T-ALL that independently proliferated in vivo used the prosurvival nuclear factor κB (NF-κB) pathway (*59*), as determined by detection of the phosphorylation of the NF-κB inhibitor protein IκBα (Fig. 6I). In two transplants with cells expressing Rasgrp1-specific shRNA, NF-κB signaling appeared to be replaced by Akt signaling (Fig. 6I), which also promotes cell survival (*54*, *56*). The PI3K-Akt pathway, which includes inhibitor signaling by phosphatase and tensin homolog deleted from chromosome 10 (PTEN), is implicated in ~50% of T-ALL patients (*60*). Furthermore, the TANK-binding kinase 1 (TKB1)–NF-κB pathway can play a critical role in various human cancers with oncogenic Ras mutations (*61*, *62*); however, currently, we do not have further evidence to substantiate a Rasgrp1–NF-κB pathway, nor do we have a molecular understanding of the how cells switch from using NF-κB signaling to using Akt signaling to survive. Thus, our panel of clonal mouse T-ALL lines retained not only a complex level of heterogeneity but also plasticity in terms of Ras effector activation. We postulate that this panel of cell lines may serve as a useful tool for future studies to further explore the heterogeneity and plasticity characteristics of Ras effector kinase pathways in patients.

DISCUSSION

We found that *RasGRP1* expression is increased in many T-ALL patients as well as in mouse T-ALLs that were caused by leukemia virus–dependent insertions in *Rasgrp1*. In contrast, *RasGRP1* expression is low in ETP T-ALL patients (*21*), and we observed no *Rasgrp1* CIS on a *K-Ras*^{G12D} mouse genetic background. We demonstrated that increased Rasgrp1 abundance resulted in only modest basal Ras activation, which did not trigger cell cycle arrest responses. Instead, our computational, biochemical, and mouse model approaches demonstrated that Rasgrp1 effectively responds to cytokine receptor input to activate Ras in T-ALL, revealing a previously uncharacterized cytokine receptor–Rasgrp1 pathway. The kinase effector pathways downstream of Ras are not "locked-in" but are highly heterogeneous in both human and murine T-ALL lines, and biochemical "rewiring" occurred in a plastic manner after perturbation of the signaling network. Reduction of Rasgrp1 retarded tumor growth, which suggests that Rasgrp1 might be an attractive target for therapies against T-ALL.

At this point, we do not know what causes the increased *RasGRP1* mRNA abundance in human T-ALL. RasGRP3 is also found in the T cell lineage, and RasGRP4 was originally isolated from acute myeloid leukemia (AML) patient complementary DNA (cDNA) (*63*), but our microarray platform with 107 T-ALL patients and the large RIM screens for T-ALL found changes only in *Rasgrp1* among the RasGRPs tested (Fig. 2). We are currently investigating the underlying mechanism for the specificity regarding *Rasgrp1*. The absolute amount of Rasgrp1 protein is relatively modest in human T-ALL lines and our murine T-ALL, even in those with the greatest amounts of *Rasgrp1* mRNA. We hypothesize that it is the dysregulation of expression rather than the absolute increase in Rasgrp1 protein abundance that contributes to leukemogenesis. In support of the regulation of expression as an important mechanism to curb Rasgrp1 function, *Rasgrp1* mRNA amounts are dynamic in thymocyte subsets (*37*) and are reduced in response to TCR stimulation (*38*), and Rasgrp1 protein abundance decreases when thymocytes mature to T cells (*40*, *41*). Indeed, even a partial reduction in Rasgrp1 abundance had a substantial effect on cytokine-induced Ras activation and proliferation of cells in vivo, suggesting that Rasgrp1 may be an attractive molecule to inhibit to interfere with cellular proliferation.

On the basis of the combined published microarray data (*19*, *25*) and our data here, we postulate that dysregulation of RasGRP1 is a common feature of human T-ALL and that it is more frequent than are oncogenic mutations in *RAS*. It is possible that signals from oncogenic Ras mutations are too strong for cells of the T lymphocyte lineage. We observed that in half of our mouse *K-Ras*^{G12D} T-ALL lines, the intrinsic Ras signal was uncoupled from the p53-p21 response. Deletion of the p53 regulators encoded by the *INK4A/ARF* locus occurs very frequently in T-ALL patients (*4*). Still, somatic mutations in *NRAS* and *KRAS* do not occur with high frequency (*18*–*20*), and perhaps dysregulation of p53 alone is not sufficient for *K-Ras*^{G12D} T-ALL to develop in patients. In support of this notion, patients with ETP T-ALL that are now known to often carry strong activating alleles, such as oncogenic *KRAS* or *NRAS* mutations or activating mutations in *IL7R*, demonstrate a very high burden of additional

cytogenetic abnormalities (*21*). Perhaps a specific set of genetic abnormalities enables the ETP T-ALL cells to proliferate despite having strong oncogenic signals that can trigger cell cycle arrest. ETP T-ALL is an aggressive malignancy that is often associated with treatment failure (*64*), and ETP T-ALL patients have low expression of *RasGRP1* (*21*). We found a strong correlation between low *RasGRP1* expression and failure to respond to treatment in two COG clinical trials with 107 pediatric T-ALL patients. Lack of available DNA prevented us from directly testing this, but it is tempting to speculate that the seven T-ALL patients that failed treatment and had very low *RasGRP1* expression instead had mutations in *KRAS* or *NRAS* and may represent cases of ETP T-ALL. Future studies need to focus on this aspect, particularly because *RasGRP1* may provide a means of stratifying patients, ideally before treatment begins.

Rasgrp1-deficient mice show a selective defect in T lymphocyte development (*65*), and Rasgrp1 and Rasgrp3 have predominantly been studied as RasGEFs that operate downstream of the TCR and BCR (*50*). Reports combined with our finding of a cytokine receptor–Rasgrp1–Ras pathway indicate that RasGEFs of the Rasgrp family also operate downstream of receptors other than the TCR and BCR. We therefore hypothesize that the concept of dysregulated RasGRP1 responding to receptor input may be more general and applicable to different types of cancer. There is some evidence for this hypothesis. For example, in a Keratin5-RasGRP1 transgenic mouse model, RasGRP1 overexpression results mostly in skin papilloma but synergizes with 12-*O*-tetradecanoylphorbol-13-acetate (TPA) treatment to stimulate the tumorigenic response (*66*). TPA is a phorbol ester that activates RasGRP1 as well as other molecules. RasGRP3 is found in a subset of human prostate and melanoma cancer samples, and RasGRP3-specific shRNA reduced hepatocyte growth factor (HGF)– or epidermal growth factor (EGF)–induced Ras signaling in prostate or melanoma cancer cell lines, as well as reduced xenograft tumor formation (*67*, *68*). Although a biochemical connection between the activation and membrane recruitment of the RasGRPs and the HGF, EGF, and cytokine receptors has not been firmly established, a role for DAG is possible. This might lead to new opportunities to interfere with oncogenic Rasgrp signals through the use of inhibitors of the PLC enzymes that produce DAG. Here, we focused on the role of Rasgrp1 downstream of the receptors for IL-2, IL-7, and IL-9 in the activation of Ras. We would like to emphasize that it is very plausible that Rasgrp1 responds to signaling by other receptors in T-ALL or that it may activate pathways other than Ras that are aberrantly triggered by increased, dysregulated Rasgrp1. These possibilities and the question of whether DAG is a prerequisite for dysregulated Rasgrp1 to be leukemogenic are important topics for future investigations. Regardless, our results indicate that Rasgrp1 itself could be a very attractive target in cancer therapy, especially because (i) our models predict that inhibition of Rasgrp1 activity below a threshold will have profound effects on Ras activation, and (ii) partial knockdown of Rasgrp1 has a noticeable effect on the proliferation of T-ALL cells.

Understanding the complexity of the Ras signaling network in T-ALL and cancer in general will be essential to guide future clinical intervention with small molecules that inhibit specific components in effector pathways downstream of Ras. We report considerable heterogeneity and plasticity in receptor-induced Ras effector pathways in either *Rasgrp1* or *K-Ras*^{G12D} T-ALL. Plausible sources of heterogeneity are different combinations of CIS, acquired or induced (ENU) mutations, and the diverse developmental stages found for T-ALL. Here, we focused mostly on the biochemical mechanism of the role of RasGRP1 in T-ALL, and we did not address the particular developmental stage(s) that Rasgrp1 might affect. Elegant application of the Sleeping Beauty system in distinct developmental subsets indicated that insertions in *Rasgrp1* leading to T-ALL typically occur in early hematopoietic subsets and often also acquire insertions in *Notch1* (*69*). These studies also initiated the interesting discussion that ETP T-ALL perhaps arises from a later developmental stage but differentiates backward (*69*, *70*).

A substantial portion (30 of 237) of SL3-3 T-ALLs with a *Rasgrp1* CIS also contain a CIS in *Notch1* (*29*). The statistical power of our large SL3-3 RIM screen supports the likelihood that both pathways complement each other and synergize in T-ALL oncogenesis. Similarly, we previously reported that oncogenic *K-Ras*^{G12D} expression from the endogenous locus cooperated with *Notch1* CIS in T lineage leukemogenesis (*39*), and 10 of 13 T-ALLs arising from retroviral-mediated *Rasgrp1* overexpression carried *Notch1* mutations (*28*). Given that mutations in *NOTCH1* are the most common oncogenic mutation in human T-ALL (*31*), it will be of interest to determine the biochemical nature of RasGRP1 and Notch1 synergy in human T-ALL. We speculate that specific sets of co-insertions might mirror the heterogeneity observed in patients. Future methodical analyses of these RIM screens and derived clonal T-ALL lines that include combined in silico, in vitro, and in vivo approaches to examine signals (preferably with single-cell resolution) might eventually reveal a blueprint of cooperating signaling networks that could help deconvolute the complexity of hyperactive Ras signaling in human cancer.

MATERIALS AND METHODS

Computational models

For Figs. 1, A and B, and 5, D and E, and fig. S1, B and C, we modeled the signaling network described in table SIV of Das *et al*. (*24*), as depicted in fig. S1A with the dotted area excluded. For Fig. 6, A, B, and F, we used the model in Fig. 1A of Riese *et al*. (*51*), which is an extended model that accounts for receptor input, as depicted in fig. S1A with the dotted area included. We performed stochastic simulations of signaling networks by solving the corresponding Master equation with the standard Gillespie algorithm (*71*). The Master equation is a probabilistic description of the time evolution of an intrinsically stochastic system governed by a set of coupled chemical reactions. We found deterministic steady-state amounts of RasGTP by finding the fixed points of the ordinary differential equations describing the system. In all stochastic simulations, we used a spatially homogeneous simulation box of size V = area (4 mm^2) × height (0.02 mm). This choice of the system size ensures that the system is well mixed. The initial concentrations and the rate constants were those in tables S1 to S4 of Das *et al*. (*24*) and Tables 1 and 2 of Riese *et al*. (*51*), except that we used 36 molecules/μm^2 for PIP_2 (phosphatidylinositol 4,5-bisphosphate) to match their published results (*51*). More details of the simulation technique and choice of parameters can be found in the supplemental materials of Das *et al*. (*24*) and Riese *et al*. (*51*).

Real-time RT-PCR

Total RNA was isolated from human bone marrow and cell lines derived from mouse leukemias with Trizol (Invitrogen) extraction according to the manufacturer's protocol. RNA was reverse-transcribed with random primers (Invitrogen) and Moloney murine leukemia virus reverse transcriptase. Real-time PCR was performed in triplicate with AmpliTaq Gold (Applied Biosystems) and the Applied Biosystems ABI 7300 thermocycler. The extents of gene expression were normalized to that of *GAPDH* and quantified with the comparative C_T method according to the manufacturer's instructions. The following combinations of primers and probes were used to analyze the expression of mouse *Rasgrp1*: forward, TGGGCTTTCCACACAACTTTC; reverse, CACCAGGTCTTTGCACTGTTTG; probe, FAM-AGAAACCACTTACCTGAAGCCCACCTTCTG-TAMRA; and human *RasGRP1*: forward, AAGCTCCACCAACTACAGAACT;

reverse, AGGGAGATGAGGTCCTTGAGAT; probe, FAM-CCACATGAAATCAATAAGGTTCTCGGTGAG-TAMRA. Notably, bone marrow samples were taken from T-ALL patients at blast crisis and consisted of a typically high percentage of blasts in the marrow (close to 100%), and these samples were therefore relatively homogeneous.

Gene expression profiling of pediatric T-ALL patients

We used the RNeasy isolation kit (Qiagen) to isolate RNA from pretreatment leukemic cell suspensions obtained from peripheral blood or bone marrow. cDNA labeling, hybridization to U133_Plus_2 arrays (Affymetrix), and scanning were performed at the Keck-UNM Genomics Resource. The default RMA and MAS5 algorithms of Expression Console (version 1.1; Affymetrix) were used to generate and normalize signal intensities, as previously described (*72*–*74*).

T-ALL clinical trials and correlative analyses

After obtaining written informed consent in accordance with local institutional guidelines, we collected peripheral blood and bone marrow from patients that were enrolled in the COG studies 9900/9404 and AALL03B1/AALL0434, and we processed and cryopreserved these samples for future tissue analyses. Failure to achieve a first remission (induction failure), relapse after achieving a first remission, and complete continuous remission were annotated for each patient. Further details regarding study design and outcome correlates are available as previously described (*74*, *75*) or at http://www.cancer.gov/clinicaltrials. Analyses of RMA-normalized data were performed with Prism 4 (GraphPad Software Inc.).

Generation and propagation of murine T-ALL cell lines

Frozen primary tumors from our previous SL3-3 screen (*29*) were thawed in complete RPMI medium (Invitrogen) containing 20% fetal bovine serum (FBS), penicillin (100 U/ml), streptomycin (100 μg/ml), 55 μM β-mercaptoethanol, and IL-2, IL-7, and IL-9 (each at 10 ng/ml), which resulted in the generation of bulk in vitro T-ALL cultures. Clonal T-ALL cell lines were then generated by limiting dilution. All T-ALL lines were subsequently propagated in RPMI, 10% FBS, containing penicillin, streptomycin, and β-mercaptoethanol. The *K-Ras*^{G12D} T-ALL 6, 3, and 51 cell lines were grown in the same medium supplemented with IL-2, IL-7, and IL-9 (each at 10 ng/ml).

In vitro stimulation and biochemical analyses

To analyze RasGTP abundance under basal conditions, we washed T-ALL lines with phosphate-buffered saline (PBS) containing magnesium and calcium and rested them in PBS for 2 hours at 37° before subjecting the cells to RasGTP pull-downs as described previously (*24*). For stimulations, cells were washed and rested in PBS for 30 min and stimulated with PMA (25 ng/ml) or with IL-2, IL-7, and IL-9 (each at 100 ng/ml), followed by RasGTP pull-downs and preparation of NP-40 lysates. NP-40 lysis buffer was supplemented with protease and phosphatase inhibitors [10 mM sodium fluoride, 2 mM sodium orthovanadate, 0.5 mM EDTA, 2 mM phenylmethylsulfonyl fluoride, 1 mM sodium molybdate, aprotonin (10 μg/ml), leupeptin (10 μg/ml), pepstatin (1 μg/ml)], and lysates were incubated for 20 min at 4°C. Western blotting analysis was performed with antibodies specific for murine Rasgrp1 (m199, a gift from J. Stone), α-tubulin (Sigma), Ras (Upstate), phosphorylated p53 at Ser^{15} (Cell Signaling), p21 (M-19, Santa Cruz Biotechnology), phosphorylated PLC-γ1 pY^{783} (Invitrogen), phosphorylated ERK1/2 (p44/42 MAPK, Cell Signaling), phosphorylated IκBα Ser^{32} (Cell Signaling), and phosphorylated Akt Ser^{473} (Cell Signaling). To detect human RasGRP1, we generated a rabbit monoclonal antibody, JR-E80-2, by immunization with GPFTFPNGEAVEHGEESKDRTIMLM-RasGRP1 peptide together with Epitomics. Western blots were visualized with enhanced chemiluminescence and imaging on a Fuji LAS 4000 image station (GE Healthcare). The protein bands in Western blots were quantified with Multi Gauge software, and densitometry (pixel intensity) was determined within the linear range of the exposure. Amounts of the proteins of interest are typically presented as a ratio of a loading control.

Measurement of in vitro proliferation of *K-Ras*^{G12D} and *Rasgrp1* T-ALL cell lines

T-ALL cell lines were seeded at 1×10^6 cells/ml in complete RPMI medium (Invitrogen) containing 10% FBS, penicillin, streptomycin, and β-mercaptoethanol; medium with 20% of the normal amount of FBS; or complete RPMI medium containing doxorubicin (100 ng/ml). Cell lines were grown with or without IL-2, IL-7, and IL-9 (each at 10 ng/ml). Samples were collected after 24, 48, 72, and 96 hours and counted with a Vi-Cell cell viability analyzer (Beckman Coulter).

Analysis of the p53-p21^{CIP} cell cycle arrest pathway

Cells (4×10^6) were harvested from T-ALL lines from in vitro growth assays after 6 and 24 hours. Samples were also collected for staining with annexin V and PI (BD Biosciences) and were processed according to the manufacturer's protocol. Cells were centrifuged and resuspended in radioimmunoprecipitation assay lysis buffer (1% NP-40, 1% sodium deoxycholate, 0.1% SDS, 50 mM Mops, 150 mM sodium chloride, 2 mM EDTA) supplemented with protease and phosphatase inhibitors. Lysates were centrifuged for 20 min at 4°C, and 2× sample buffer was added to the supernatants. Protein samples were separated on a precast 4 to 12% gradient gel (Invitrogen) for P-p53 and p21 analysis.

In vivo proliferation of *K-Ras*^{G12D} and *Rasgrp1* T-ALL lines

T-ALL cells (1×10^5) were injected subcutaneously into Nude-*Foxn1*^{nu} mice (Harlan). Tumor volume was determined by external caliper measurement and calculated as follows: tumor volume = $^1/_2$ (length × width^2). Mice were monitored and euthanized once adverse effects were observed. Tumors were removed and single-cell suspensions were prepared for protein and RNA extraction. Cells were resuspended in NP-40 lysis buffer supplemented with protease and phosphatase inhibitors and incubated at 4°C for 20 min. Lysates were centrifuged at 4°C for 20 min, and sample buffer was added to the supernatants. Proteins were separated on a 10% SDS-polyacrylamide gel and were analyzed by Western blotting. Mice were handled according to the Institutional Animal Care and Use Committee regulations, described in the Roose laboratory UCSF (University of California, San Francisco) mouse protocol AN084051 "Ras Signal Transduction in Lymphocytes and Cancer."

shRNA experiments

Oligonucleotides containing Hap I and Xho I sites were annealed and ligated into Hap 1– and Xho I–digested pSicoR-puro-t2a-eGFP to create mRasgrp1-1503–pSicoR-puro-t2a-eGFP and hRasGRP1-1503–pSicoR-puro-t2a-eGFP. The oligonucleotide sequences are as follows. For mRasgrp1-1503: sense oligonucleotide, 5′-TGATCGCTGCAAGCTTTCCATTCAAGAGATGGAAAGCTTGCAGCGATCTTTTTTC-3′; antisense oligonucleotide, 5′-TCGAGAAAAAAGATCGCTGCAAGCTTTCCATCTCTTGAATGGAAAGCTTGCAGCGATCA-3′. For hRasGRP1-1503: sense oligonucleotide, 5′-TGAT***T***GCTGC***G***AG***T***TTTCCATTCAAGAGATGGAAAACTCGCAGCAATCTTTTTTC-3′; antisense oligonucleotide, 5′-TCGAGAAAAAAGATTGCTGCGAGTTTTCCATCTCTTGAATGGAAAACTCGCAGCAATCA-3′. Targeting of the 1503 region was based on previous work (*76*). hRasGRP1-1503 targets human RasGRP1, has three mismatches with the same sequence in mRasgrp1-1503, and

served as a specificity control. Clonal T-ALL lines were infected with lentivirus through standard spin infections and selected by culture in the presence of puromycin (0.5 μg/ml). Similarly, annealed oligonucleotides were ligated into pSicoR-puro-t2a-eGFP to create mSos1-1313–pSicoR-puro-t2a-eGFP and hSOS1-1313–pSicoR-puro-t2a-eGFP, based on published targeting sequences (*77*). hSOS1-1313 targets human SOS1, has two mismatches with the same sequence in mSos1-1313, and served as a specificity control. For mSos1-1313: sense oligonucleotide, 5′-TGACAGTGTTGCAATGAGTTTTCAAGAGAAACTCATTGCAACACTGTCTTTTTTC-3′; antisense oligonucleotide, 5′-TCGAGAAAAAAGACAGTGTTGCAATGAGTTTCTCTTGAAAACTCATTGCAACACTGTCA-3′. For hSOS1-1313: sense oligonucleotide, 5′-TGACAGTGTTG*T*TAATGA*A*TTTTCAAGAGAAATTCATTACAACACTGTCTTTTTTC-3′; antisense oligonucleotide, 5′-TCGAGAAAAAAGACAGTGTTGTAATGAATTTCTCTTGAAAATTCATTACAACACTGTCA-3′.

In vivo comparison of *Rasgrp1* T-ALL cells and *Rasgrp1* T-ALL cells containing Rasgrp1-specific shRNA

BALB/c mice (Harlan) were injected with 4×10^3 *Rasgrp1* or shRNA *Rasgrp1* T-ALL cells by retro-orbital injection. Mice were euthanized after 14 days, and lymph nodes, spleen, liver, thymus, lungs, kidneys, and femurs were removed. Single-cell suspensions were prepared and analyzed to determine the percentage of GFP^+ cells present in each tissue by flow cytometry. Unpaired Student's *t* tests were applied to explore the effects of Rasgrp1 knockdown.

Sternums and livers were fixed in 10% buffer formalin (Fisher Scientific) for 24 hours and maintained in 70% ethanol at 4°C until they were embedded in paraffin. Paraffin-embedded sections (10 μm) were stained with H&E or with anti-Rasgrp1 antibody (Abcam, 37927) to detect Rasgrp1 abundance, and slides were used for descriptive histopathology. Briefly, slides were deparaffinized and rehydrated followed by antigen retrieval in Trilogy buffer (Cell Marque) at 90°C for 45 min. Slides were washed in PBS-T (0.1% Tween 20 in PBS), blocked with blocking buffer [50 mM tris-HCl (pH 7.6) containing 1% bovine serum albumin], and stained with primary antibody (rabbit anti-RasGRP1 antibody at 1:500 dilution) overnight at 4°C. After being washed with PBS-T, slides were incubated with Alexa Fluor 488–conjugated donkey anti-rabbit antibody (Invitrogen, 1:1000) for 50 min at room temperature. Slides were washed and mounted with Vectashield mounting medium (Vector Laboratories).

SUPPLEMENTARY MATERIALS

www.sciencesignaling.org/cgi/content/full/6/268/ra21/DC1

Fig. S1. Computational models to explore T-ALL Ras activation.
Fig. S2. Overview of the *Rasgrp1* viral insertion map.
Fig. S3. Characterization of T-ALL cell lines used in this study.
Fig. S4. Analysis of p53 phosphorylation, p21 abundance, and the extent of apoptosis in *Rasgrp1* and *K-Ras*^{G12D} T-ALL lines.
Fig. S5. In vitro proliferation of *K-Ras*^{G12D} and *Rasgrp1* T-ALL lines.
Fig. S6. In vivo proliferation of *K-Ras*^{G12D} and *Rasgrp1* T-ALL cell lines.
Fig. S7. Rasgrp1 abundance in 3397S-E and 1156S-O cells, and cell-survival characteristics and Rasgrp1 abundance in 1156S-O *Rasgrp1* T-ALL transplants.
Fig. S8. PMA-induced ERK phosphorylation in *K-Ras*^{G12D} and *Rasgrp1* T-ALL cell lines.

REFERENCES AND NOTES

1. C. H. Pui, M. V. Relling, J. R. Downing, Acute lymphoblastic leukemia. *N. Engl. J. Med.* **350**, 1535–1548 (2004).
2. C. H. Pui, W. E. Evans, Treatment of acute lymphoblastic leukemia. *N. Engl. J. Med.* **354**, 166–178 (2006).
3. S. Bhatia, H. N. Sather, O. B. Pabustan, M. E. Trigg, P. S. Gaynon, L. L. Robison, Low incidence of second neoplasms among children diagnosed with acute lymphoblastic leukemia after 1983. *Blood* **99**, 4257–4264 (2002).
4. C. Graux, J. Cools, L. Michaux, P. Vandenberghe, A. Hagemeijer, Cytogenetics and molecular genetics of T-cell acute lymphoblastic leukemia: From thymocyte to lymphoblast. *Leukemia* **20**, 1496–1510 (2006).
5. S. A. Armstrong, A. T. Look, Molecular genetics of acute lymphoblastic leukemia. *J. Clin. Oncol.* **23**, 6306–6315 (2005).
6. I. Aifantis, E. Raetz, S. Buonamici, Molecular pathogenesis of T-cell leukaemia and lymphoma. *Nat. Rev.* **8**, 380–390 (2008).
7. C. Grabher, H. von Boehmer, A. T. Look, Notch 1 activation in the molecular pathogenesis of T-cell acute lymphoblastic leukaemia. *Nat. Rev. Cancer* **6**, 347–359 (2006).
8. A. A. Ferrando, D. S. Neuberg, J. Staunton, M. L. Loh, C. Huard, S. C. Raimondi, F. G. Behm, C. H. Pui, J. R. Downing, D. G. Gilliland, E. S. Lander, T. R. Golub, A. T. Look, Gene expression signatures define novel oncogenic pathways in T cell acute lymphoblastic leukemia. *Cancer Cell* **1**, 75–87 (2002).
9. L. M. Staudt, S. Dave, The biology of human lymphoid malignancies revealed by gene expression profiling. *Adv. Immunol.* **87**, 163–208 (2005).
10. E. Thiel, B. R. Kranz, A. Raghavachar, C. R. Bartram, H. Löffler, D. Messerer, A. Ganser, W. D. Ludwig, T. Büchner, D. Hoelzer, Prethymic phenotype and genotype of pre-T (CD7+/ER–)-cell leukemia and its clinical significance within adult acute lymphoblastic leukemia. *Blood* **73**, 1247–1258 (1989).
11. J. Pullen, J. J. Shuster, M. Link, M. Borowitz, M. Amylon, A. J. Carroll, V. Land, A. T. Look, B. McIntyre, B. Camitta, Significance of commonly used prognostic factors differs for children with T cell acute lymphocytic leukemia (ALL), as compared to those with B-precursor ALL. A Pediatric Oncology Group (POG) study. *Leukemia* **13**, 1696–1707 (1999).
12. C. H. Pui, M. L. Hancock, D. R. Head, G. K. Rivera, A. T. Look, J. T. Sandlund, F. G. Behm, Clinical significance of CD34 expression in childhood acute lymphoblastic leukemia. *Blood* **82**, 889–894 (1993).
13. F. C. von Lintig, I. Huvar, P. Law, M. B. Diccianni, A. L. Yu, G. R. Boss, Ras activation in normal white blood cells and childhood acute lymphoblastic leukemia. *Clin. Cancer Res.* **6**, 1804–1810 (2000).
14. L. Buday, J. Downward, Many faces of Ras activation. *Biochim. Biophys. Acta* **1786**, 178–187 (2008).
15. D. Vigil, J. Cherfils, K. L. Rossman, C. J. Der, Ras superfamily GEFs and GAPs: Validated and tractable targets for cancer therapy? *Nat. Rev. Cancer* **10**, 842–857 (2010).
16. J. L. Bos, *ras* oncogenes in human cancer: A review. *Cancer Res.* **49**, 4682–4689 (1989).
17. P. H. Seeburg, W. W. Colby, D. J. Capon, D. V. Goeddel, A. D. Levinson, Biological properties of human c-Ha-*ras*1 genes mutated at codon 12. *Nature* **312**, 71–75 (1984).
18. H. G. Ahuja, A. Foti, M. Bar-Eli, M. J. Cline, The pattern of mutational involvement of RAS genes in human hematologic malignancies determined by DNA amplification and direct sequencing. *Blood* **75**, 1684–1690 (1990).
19. E. J. Yeoh, M. E. Ross, S. A. Shurtleff, W. K. Williams, D. Patel, R. Mahfouz, F. G. Behm, S. C. Raimondi, M. V. Relling, A. Patel, C. Cheng, D. Campana, D. Wilkins, X. Zhou, J. Li, H. Liu, C. H. Pui, W. E. Evans, C. Naeve, L. Wong, J. R. Downing, Classification, subtype discovery, and prediction of outcome in pediatric acute lymphoblastic leukemia by gene expression profiling. *Cancer Cell* **1**, 133–143 (2002).
20. J. L. Wiemels, Y. Zhang, J. Chang, S. Zheng, C. Metayer, L. Zhang, M. T. Smith, X. Ma, S. Selvin, P. A. Buffler, J. K. Wiencke, *RAS* mutation is associated with hyperdiploidy and parental characteristics in pediatric acute lymphoblastic leukemia. *Leukemia* **19**, 415–419 (2005).
21. J. Zhang, L. Ding, L. Holmfeldt, G. Wu, S. L. Heatley, D. Payne-Turner, J. Easton, X. Chen, J. Wang, M. Rusch, C. Lu, S. C. Chen, L. Wei, J. R. Collins-Underwood, J. Ma, K. G. Roberts, S. B. Pounds, A. Ulyanov, J. Becksfort, P. Gupta, R. Huether, R. W. Kriwacki, M. Parker, D. J. McGoldrick, D. Zhao, D. Alford, S. Espy, K. C. Bobba, G. Song, D. Pei, C. Cheng, S. Roberts, M. I. Barbato, D. Campana, E. Coustan-Smith, S. A. Shurtleff, S. C. Raimondi, M. Kleppe, J. Cools, K. A. Shimano, M. L. Hermiston, S. Doulatov, K. Eppert, E. Laurenti, F. Notta, J. E. Dick, G. Basso, S. P. Hunger, M. L. Loh, M. Devidas, B. Wood, S. Winter, K. P. Dunsmore, R. S. Fulton, L. L. Fulton, X. Hong, C. C. Harris, D. J. Dooling, K. Ochoa, K. J. Johnson, J. C. Obenauer, W. E. Evans, C. H. Pui, C. W. Naeve, T. J. Ley, E. R. Mardis, R. K. Wilson, J. R. Downing, C. G. Mullighan, The genetic basis of early T-cell precursor acute lymphoblastic leukaemia. *Nature* **481**, 157–163 (2012).
22. P. P. Zenatti, D. Ribeiro, W. Li, L. Zuurbier, M. C. Silva, M. Paganin, J. Tritapoe, J. A. Hixon, A. B. Silveira, B. A. Cardoso, L. M. Sarmento, N. Correia, M. L. Toribio, J. Kobarg, M. Horstmann, R. Pieters, S. R. Brandalise, A. A. Ferrando, J. P. Meijerink, S. K. Durum, J. A. Yunes, J. T. Barata, Oncogenic *IL7R* gain-of-function mutations in childhood T-cell acute lymphoblastic leukemia. *Nat. Genet.* **43**, 932–939 (2011).
23. A. Silva, A. B. Laranjeira, L. R. Martins, B. A. Cardoso, J. Demengeot, J. A. Yunes, B. Seddon, J. T. Barata, IL-7 contributes to the progression of human T-cell acute lymphoblastic leukemias. *Cancer Res.* **71**, 4780–4789 (2011).
24. J. Das, M. Ho, J. Zikherman, C. Govern, M. Yang, A. Weiss, A. K. Chakraborty, J. P. Roose, Digital signaling and hysteresis characterize ras activation in lymphoid cells. *Cell* **136**, 337–351 (2009).

25. T. Sanda, X. Li, A. Gutierrez, Y. Ahn, D. S. Neuberg, J. O'Neil, P. R. Strack, C. G. Winter, S. S. Winter, R. S. Larson, H. von Boehmer, A. T. Look, Interconnecting molecular pathways in the pathogenesis and drug sensitivity of T-cell acute lymphoblastic leukemia. *Blood* **115**, 1735–1745 (2010).
26. T. Palomero, M. L. Sulis, M. Cortina, P. J. Real, K. Barnes, M. Ciofani, E. Caparros, J. Buteau, K. Brown, S. L. Perkins, G. Bhagat, A. M. Agarwal, G. Basso, M. Castillo, S. Nagase, C. Cordon-Cardo, R. Parsons, J. C. Zúñiga-Pflücker, M. Dominguez, A. A. Ferrando, Mutational loss of PTEN induces resistance to NOTCH1 inhibition in T-cell leukemia. *Nat. Med.* **13**, 1203–1210 (2007).
27. Y. Sandberg, E. J. van Gastel-Mol, B. Verhaaf, K. H. Lam, J. J. van Dongen, A. W. Langerak, BIOMED-2 multiplex immunoglobulin/T-cell receptor polymerase chain reaction protocols can reliably replace Southern blot analysis in routine clonality diagnostics. *J. Mol. Diagn.* **7**, 495–503 (2005).
28. T. Oki, J. Kitaura, N. Watanabe-Okochi, K. Nishimura, A. Maehara, T. Uchida, Y. Komeno, F. Nakahara, Y. Harada, T. Sonoki, H. Harada, T. Kitamura, Aberrant expression of RasGRP1 cooperates with gain-of-function NOTCH1 mutations in T-cell leukemogenesis. *Leukemia* **26**, 1038–1045 (2012).
29. G. B. Beck-Engeser, A. M. Lum, K. Huppi, N. J. Caplen, B. B. Wang, M. Wabl, *Pvt1*-encoded microRNAs in oncogenesis. *Retrovirology* **5**, 4 (2008).
30. Y. W. Lin, R. A. Nichols, J. J. Letterio, P. D. Aplan, *Notch1* mutations are important for leukemic transformation in murine models of precursor-T leukemia/lymphoma. *Blood* **107**, 2540–2543 (2006).
31. A. P. Weng, A. A. Ferrando, W. Lee, J. P. Morris IV, L. B. Silverman, C. Sanchez-Irizarry, S. C. Blacklow, A. T. Look, J. C. Aster, Activating mutations of *NOTCH1* in human T cell acute lymphoblastic leukemia. *Science* **306**, 269–271 (2004).
32. B. V. Balgobind, P. Van Vlierberghe, A. M. van den Ouweland, H. B. Beverloo, J. N. Terlouw-Kromosoeto, E. R. van Wering, D. Reinhardt, M. Horstmann, G. J. Kaspers, R. Pieters, C. M. Zwaan, M. M. Van den Heuvel-Eibrink, J. P. Meijerink, Leukemia-associated *NF1* inactivation in patients with pediatric T-ALL and AML lacking evidence for neurofibromatosis. *Blood* **111**, 4322–4328 (2008).
33. H. Mikkers, J. Allen, P. Knipscheer, L. Romeijn, A. Hart, E. Vink, A. Berns, High-throughput retroviral tagging to identify components of specific signaling pathways in cancer. *Nat. Genet.* **32**, 153–159 (2002).
34. K. Akagi, T. Suzuki, R. M. Stephens, N. A. Jenkins, N. G. Copeland, RTCGD: Retroviral tagged cancer gene database. *Nucleic Acids Res.* **32**, D523–D527 (2004).
35. T. Suzuki, H. Shen, K. Akagi, H. C. Morse, J. D. Malley, D. Q. Naiman, N. A. Jenkins, N. G. Copeland, New genes involved in cancer identified by retroviral tagging. *Nat. Genet.* **32**, 166–174 (2002).
36. M. B. Klinger, B. Guilbault, R. E. Goulding, R. J. Kay, Deregulated expression of RasGRP1 initiates thymic lymphomagenesis independently of T-cell receptors. *Oncogene* **24**, 2695–2704 (2005).
37. A. M. Norment, L. Y. Bogatzki, M. Klinger, E. W. Ojala, M. J. Bevan, R. J. Kay, Transgenic expression of RasGRP1 induces the maturation of double-negative thymocytes and enhances the production of CD8 single-positive thymocytes. *J. Immunol.* **170**, 1141–1149 (2003).
38. M. Diehn, A. A. Alizadeh, O. J. Rando, C. L. Liu, K. Stankunas, D. Botstein, G. R. Crabtree, P. O. Brown, Genomic expression programs and the integration of the CD28 costimulatory signal in T cell activation. *Proc. Natl. Acad. Sci. U.S.A.* **99**, 11796–11801 (2002).
39. M. Dail, Q. Li, A. McDaniel, J. Wong, K. Akagi, B. Huang, H. C. Kang, S. C. Kogan, K. Shokat, L. Wolff, B. S. Braun, K. Shannon, Mutant *Ikzf1*, *Kras*^{G12D}, and *Notch1* cooperate in T lineage leukemogenesis and modulate responses to targeted agents. *Proc. Natl. Acad. Sci. U.S.A.* **107**, 5106–5111 (2010).
40. J. J. Priatel, S. J. Teh, N. A. Dower, J. C. Stone, H. S. Teh, RasGRP1 transduces low-grade TCR signals which are critical for T cell development, homeostasis, and differentiation. *Immunity* **17**, 617–627 (2002).
41. R. L. Kortum, C. L. Sommers, C. P. Alexander, J. M. Pinski, W. Li, A. Grinberg, J. Lee, P. E. Love, L. E. Samelson, Targeted Sos1 deletion reveals its critical role in early T-cell development. *Proc. Natl. Acad. Sci. U.S.A.* **108**, 12407–12412 (2011).
42. S. W. Lowe, E. Cepero, G. Evan, Intrinsic tumour suppression. *Nature* **432**, 307–315 (2004).
43. J. Campisi, Senescent cells, tumor suppression, and organismal aging: Good citizens, bad neighbors. *Cell* **120**, 513–522 (2005).
44. J. C. Renauld, N. van der Lugt, A. Vink, M. van Roon, C. Godfraind, G. Warnier, H. Merz, A. Feller, A. Berns, J. Van Snick, Thymic lymphomas in interleukin 9 transgenic mice. *Oncogene* **9**, 1327–1332 (1994).
45. B. E. Rich, J. Campos-Torres, R. I. Tepper, R. W. Moreadith, P. Leder, Cutaneous lymphoproliferation and lymphomas in interleukin 7 transgenic mice. *J. Exp. Med.* **177**, 305–316 (1993).
46. J. T. Barata, A. A. Cardoso, V. A. Boussiotis, Interleukin-7 in T-cell acute lymphoblastic leukemia: An extrinsic factor supporting leukemogenesis? *Leuk. Lymphoma* **46**, 483–495 (2005).
47. J. T. Barata, T. D. Keenan, A. Silva, L. M. Nadler, V. A. Boussiotis, A. A. Cardoso, Common γ chain-signaling cytokines promote proliferation of T-cell acute lymphoblastic leukemia. *Haematologica* **89**, 1459–1467 (2004).
48. D. E. Levy, J. E. Darnell Jr., STATs: Transcriptional control and biological impact. *Nat. Rev. Mol. Cell Biol.* **3**, 651–662 (2002).
49. S. N. Constantinescu, M. Girardot, C. Pecquet, Mining for JAK-STAT mutations in cancer. *Trends Biochem. Sci.* **33**, 122–131 (2008).
50. J. C. Stone, Regulation of Ras in lymphocytes: Get a GRP. *Biochem. Soc. Trans.* **34**, 858–861 (2006).
51. M. J. Riese, J. Grewal, J. Das, T. Zou, V. Patil, A. K. Chakraborty, G. A. Koretzky, Decreased diacylglycerol metabolism enhances ERK activation and augments CD8$^+$ T cell functional responses. *J. Biol. Chem.* **286**, 5254–5265 (2011).
52. J. P. Roose, M. Mollenauer, M. Ho, T. Kurosaki, A. Weiss, Unusual interplay of two types of Ras activators, RasGRP and SOS, establishes sensitive and robust Ras activation in lymphocytes. *Mol. Cell. Biol.* **27**, 2732–2745 (2007).
53. S. Boykevisch, C. Zhao, H. Sondermann, P. Philippidou, S. Halegoua, J. Kuriyan, D. Bar-Sagi, Regulation of Ras signaling dynamics by Sos-mediated positive feedback. *Curr. Biol.* **16**, 2173–2179 (2006).
54. S. Schubbert, K. Shannon, G. Bollag, Hyperactive Ras in developmental disorders and cancer. *Nat. Rev. Cancer* **7**, 295–308 (2007).
55. A. Prasad, J. Zikherman, J. Das, J. P. Roose, A. Weiss, A. K. Chakraborty, Origin of the sharp boundary that discriminates positive and negative selection of thymocytes. *Proc. Natl. Acad. Sci. U.S.A.* **106**, 528–533 (2009).
56. J. Downward, Cancer biology: Signatures guide drug choice. *Nature* **439**, 274–275 (2006).
57. K. Scheffzek, M. R. Ahmadian, W. Kabsch, L. Wiesmüller, A. Lautwein, F. Schmitz, A. Wittinghofer, The Ras-RasGAP complex: Structural basis for GTPase activation and its loss in oncogenic Ras mutants. *Science* **277**, 333–338 (1997).
58. R. S. Maser, B. Choudhury, P. J. Campbell, B. Feng, K. K. Wong, A. Protopopov, J. O'Neil, A. Gutierrez, E. Ivanova, I. Perna, E. Lin, V. Mani, S. Jiang, K. McNamara, S. Zaghlul, S. Edkins, C. Stevens, C. Brennan, E. S. Martin, R. Wiedemeyer, O. Kabbarah, C. Nogueira, G. Histen, J. Aster, M. Mansour, V. Duke, L. Foroni, A. K. Fielding, A. H. Goldstone, J. M. Rowe, Y. A. Wang, A. T. Look, M. R. Stratton, L. Chin, P. A. Futreal, R. A. DePinho, Chromosomally unstable mouse tumours have genomic alterations similar to diverse human cancers. *Nature* **447**, 966–971 (2007).
59. M. S. Hayden, S. Ghosh, Signaling to NF-κB. *Genes Dev.* **18**, 2195–2224 (2004).
60. A. Gutierrez, T. Sanda, R. Grebliunaite, A. Carracedo, L. Salmena, Y. Ahn, S. Dahlberg, D. Neuberg, L. A. Moreau, S. S. Winter, R. Larson, J. Zhang, A. Protopopov, L. Chin, P. P. Pandolfi, L. B. Silverman, S. P. Hunger, S. E. Sallan, A. T. Look, High frequency of *PTEN*, *PI3K*, and *AKT* abnormalities in T-cell acute lymphoblastic leukemia. *Blood* **114**, 647–650 (2009).
61. E. Meylan, A. L. Dooley, D. M. Feldser, L. Shen, E. Turk, C. Ouyang, T. Jacks, Requirement for NF-κB signalling in a mouse model of lung adenocarcinoma. *Nature* **462**, 104–107 (2009).
62. D. A. Barbie, P. Tamayo, J. S. Boehm, S. Y. Kim, S. E. Moody, I. F. Dunn, A. C. Schinzel, P. Sandy, E. Meylan, C. Scholl, S. Fröhling, E. M. Chan, M. L. Sos, K. Michel, C. Mermel, S. J. Silver, B. A. Weir, J. H. Reiling, Q. Sheng, P. B. Gupta, R. C. Wadlow, H. Le, S. Hoersch, B. S. Wittner, S. Ramaswamy, D. M. Livingston, D. M. Sabatini, M. Meyerson, R. K. Thomas, E. S. Lander, J. P. Mesirov, D. E. Root, D. G. Gilliland, T. Jacks, W. C. Hahn, Systematic RNA interference reveals that oncogenic *KRAS*-driven cancers require TBK1. *Nature* **462**, 108–112 (2009).
63. G. W. Reuther, Q. T. Lambert, J. F. Rebhun, M. A. Caligiuri, L. A. Quilliam, C. J. Der, RasGRP4 is a novel Ras activator isolated from acute myeloid leukemia. *J. Biol. Chem.* **277**, 30508–30514 (2002).
64. E. Coustan-Smith, C. G. Mullighan, M. Onciu, F. G. Behm, S. C. Raimondi, D. Pei, C. Cheng, X. Su, J. E. Rubnitz, G. Basso, A. Biondi, C. H. Pui, J. R. Downing, D. Campana, Early T-cell precursor leukaemia: A subtype of very high-risk acute lymphoblastic leukaemia. *Lancet Oncol.* **10**, 147–156 (2009).
65. N. A. Dower, S. L. Stang, D. A. Bottorff, J. O. Ebinu, P. Dickie, H. L. Ostergaard, J. C. Stone, RasGRP is essential for mouse thymocyte differentiation and TCR signaling. *Nat. Immunol.* **1**, 317–321 (2000).
66. C. T. Luke, C. E. Oki-Idouchi, J. M. Cline, P. S. Lorenzo, RasGRP1 overexpression in the epidermis of transgenic mice contributes to tumor progression during multistage skin carcinogenesis. *Cancer Res.* **67**, 10190–10197 (2007).
67. D. Yang, N. Kedei, L. Li, J. Tao, J. F. Velasquez, A. M. Michalowski, B. I. Tóth, R. Marincsák, A. Varga, T. Biró, S. H. Yuspa, P. M. Blumberg, RasGRP3 contributes to formation and maintenance of the prostate cancer phenotype. *Cancer Res.* **70**, 7905–7917 (2010).
68. D. Yang, J. Tao, L. Li, N. Kedei, Z. E. Toth, A. Czap, J. F. Velasquez, D. Mihova, A. M. Michalowski, S. H. Yuspa, P. M. Blumberg, RasGRP3, a Ras activator, contributes to signaling and the tumorigenic phenotype in human melanoma. *Oncogene* **30**, 4590–4600 (2011).
69. K. E. Berquam-Vrieze, K. Nannapaneni, B. T. Brett, L. Holmfeldt, J. Ma, O. Zagorodna, N. A. Jenkins, N. G. Copeland, D. K. Meyerholz, C. M. Knudson, C. G. Mullighan, T. E. Scheetz, A. J. Dupuy, Cell of origin strongly influences genetic selection in a mouse model of T-ALL. *Blood* **118**, 4646–4656 (2011).
70. M. Dose, F. Gounari, Sleeping Beauty: Does ETP-ALL awaken later? *Blood* **118**, 4500–4501 (2011).

71. D. T. Gillespie, Exact stochastic simulation of coupled chemical reactions. *J. Phys. Chem.* **81**, 2340–2361 (1977).
72. R. C. Harvey, C. G. Mullighan, I. M. Chen, W. Wharton, F. M. Mikhail, A. J. Carroll, H. Kang, W. Liu, K. K. Dobbin, M. A. Smith, W. L. Carroll, M. Devidas, W. P. Bowman, B. M. Camitta, G. H. Reaman, S. P. Hunger, J. R. Downing, C. L. Willman, Rearrangement of *CRLF2* is associated with mutation of *JAK* kinases, alteration of *IKZF1*, Hispanic/Latino ethnicity, and a poor outcome in pediatric B-progenitor acute lymphoblastic leukemia. *Blood* **115**, 5312–5321 (2010).
73. H. Kang, C. S. Wilson, R. C. Harvey, I. M. Chen, M. H. Murphy, S. R. Atlas, E. J. Bedrick, M. Devidas, A. J. Carroll, B. W. Robinson, R. W. Stam, M. G. Valsecchi, R. Pieters, N. A. Heerema, J. M. Hilden, C. A. Felix, G. H. Reaman, B. Camitta, N. Winick, W. L. Carroll, Z. E. Dreyer, S. P. Hunger, C. L. Willman, Gene expression profiles predictive of outcome and age in infant acute lymphoblastic leukemia: A Children's Oncology Group study. *Blood* **119**, 1872–1881 (2012).
74. S. S. Winter, Z. Jiang, H. M. Khawaja, T. Griffin, M. Devidas, B. L. Asselin, R. S. Larson; Children's Oncology Group, Identification of genomic classifiers that distinguish induction failure in T-lineage acute lymphoblastic leukemia: A report from the Children's Oncology Group. *Blood* **110**, 1429–1438 (2007).
75. B. L. Asselin, M. Devidas, C. Wang, J. Pullen, M. J. Borowitz, R. Hutchison, S. E. Lipshultz, B. M. Camitta, Effectiveness of high-dose methotrexate in T-cell lymphoblastic leukemia and advanced-stage lymphoblastic lymphoma: A randomized study by the Children's Oncology Group (POG 9404). *Blood* **118**, 874–883 (2011).
76. J. P. Roose, M. Mollenauer, V. A. Gupta, J. Stone, A. Weiss, A diacylglycerol-protein kinase C-RasGRP1 pathway directs Ras activation upon antigen receptor stimulation of T cells. *Mol. Cell. Biol.* **25**, 4426–4441 (2005).
77. H. S. Hwang, S. G. Hwang, J. H. Cho, J. S. Chae, K. W. Yoon, S. G. Cho, E. J. Choi, CIIA functions as a molecular switch for the Rac1-specific GEF activity of SOS1. *J. Cell Biol.* **195**, 377–386 (2011).

Acknowledgments: We thank M. Krummel for 55 and 98 cell lines, G. Evan and M. Juntilla for assistance with the p53-p21 assays, A. Ferrando for human T-ALL lines, J. Stone for m199 and m133 hybridoma cell lines, and M. Hermiston, Z. Werb, and J. Stone for critical reading of the manuscript. **Funding:** This work was supported by a Director's Pioneer award (to A.K.C.), the Sidney Kimmel Foundation (to J.P.R.), the Gabrielle's Angel Foundation (to J.P.R.), the Sandler Program in Basic Science (start-up to J.P.R.), National Cancer Institute U54CA143874 Physical Science Oncology Center (PSOC to K.S., A.K.C., and J.P.R.), PO1 AI091580 (to A.K.C. and J.P.R.), R01AI041570 (to M.W.), R37CA72614 (to K.S.), K99CA157950 (to M.D.), and R01 5CA114589-07 (to S.S.W.). K.S. is an American Cancer Society Research Professor. **Author contributions:** C.H., O.K., and E.L. designed the research and performed most of the molecular, biochemical, and in vivo studies with assistance from J.B., T.L.L., and A.B. and wrote part of the paper; K.C. characterized a portion of the T-ALL cell lines and developed the shRNA. M.Y. and C.G. performed the computational simulations under the mentorship of A.K.C.; M.D. and K.A. provided reagents; R.C.H. and S.S.W. performed *RasGRP1* expression analyses on patients; M.W. provided critical mouse T-ALL reagents; S.S.W., M.L., K.S., A.K.C., and M.W. provided stimulating discussions; and J.P.R. conceived the work, wrote the paper, and supervised the work. **Competing interests:** The authors declare that they have no competing interests.

Submitted 5 December 2012
Accepted 7 March 2013
Final Publication 26 March 2013
10.1126/scisignal.2003848
Citation: C. Hartzell, O. Ksionda, E. Lemmens, K. Coakley, M. Yang, M. Dail, R. C. Harvey, C. Govern, J. Bakker, T. L. Lenstra, K. Ammon, A. Boeter, S. S. Winter, M. Loh, K. Shannon, A. K. Chakraborty, M. Wabl, J. P. Roose, Dysregulated RasGRP1 responds to cytokine receptor input in T cell leukemogenesis. *Sci. Signal.* **6**, ra21 (2013).